



Title	Lithium-containing S-PRG fillers promoted wound healing process of pulp tissues through activation of Wnt/ β -catenin signaling pathway
Author(s)	Ali Saeed Ali, Manahil
Citation	大阪大学, 2020, 博士論文
Version Type	VoR
URL	https://doi.org/10.18910/76296
rights	
Note	

The University of Osaka Institutional Knowledge Archive : OUKA

<https://ir.library.osaka-u.ac.jp/>

The University of Osaka

**Lithium-containing S-PRG fillers promoted the wound
healing process of pulp tissues through activation of
Wnt/ β -catenin signaling pathway**

Manahil Ali Saeed Ali

Ph.D. Dissertation (2016 – 2020)

Osaka University Graduate School of Dentistry

Course for Molecular Oral Biology and Dentistry

Department of Restorative Dentistry and Endodontology

Supervisor: Professor Mikako Hayashi

Acknowledgement

To my dear parents who loved, praised, and encouraged me, I have reached this stage in my life because of you, and words will not be enough to express my respect, gratitude, and love for them.

To all my sisters, brothers, and friends, thank you for always being beside me. Also, a warm heartfelt gratitude to the head of the Restorative Department and Endodontology, Professor Hayashi Mikako, who provided me the chance to pursue this doctoral program. Further, a wholehearted special thanks to my dear supervisor Dr. Takahashi Yusuke, who supervised my work and guided me through this entire journey. Further, I thank Dr. Okamoto Motoki, who directed and taught me my first steps and who continued to advise and encourage me whenever I needed them.

I would also like to thank my group members for their kind support and assistance.

Special thanks to the reviewer committee who revised and commented on my work. To Professor Kawabata Shigetada, Dr. Kuboniwa Masae and Dr. Nishibe Mariko, your pieces of advice and suggestions were essential and beneficial in the completion of my work, and I learned a lot from you.

To the members of SHOFU Inc., Mr. Nakatsuka and Mr. Sakamoto, thank you for your consistent support and material provision. You ensured the smooth proceeding of my experiments.

I thank the Japanese Government for facilitating my living and thus, completion of this project over the past 5 years. Every moment I lived here will be engraved in my memory. I had many valuable experiences that made me stronger, wiser, and more prepared for the next chapter of my life.

Thank you, Allah, for always being here, helping me reach the stars and protecting me by your kindness and strength.

This thesis is the ending of one chapter, but the beginning of another.

Sincerely,

Manahil Ali

March, 2020

INDEX

Abbreviations	8
Abstract	9
<u>Chapter I</u>	<u>Introduction</u>
1. Introduction	10
2. Hypothesis	14
3. Objectives	15
4. Significance of the study	16
5. Conflict of interest	16
<u>Chapter II</u>	<u>Materials and methods</u>
1. Materials	17
2. Methods	
2.1. Animal experiment:	18
2.1.1. Direct pulp capping procedure	18
2.1.2. Micro-computed tomography and histopathological evaluation	19
2.1.3. Masson tri-chrome staining	20
3. <i>In vitro</i> experiments:	

3.1. Mechanical properties:	21
3.1.1. Compressive and shear bond strength	21
3.1.2. Preparation of eluates and measurements of released ions	21
3.2. Cell studies:	
3.2.1. Viable cell counting	22
3.2.2. Cytotoxicity assay	23
3.2.3. Cell migration assay (wound healing technique)	23
3.2.4. Alkaline phosphatase staining assay	24
3.2.5. Alizarin red staining assay	24
4. <i>In vivo</i> assessment of Wnt/B-catenin signaling activation	
4.1. Fluorescent immunohistochemistry staining	25
5. Comparative study for various properties of lithium containing S-PRG cement	
5.1. Disk preparation	26
5.1.1. Hydroxyapatite formation assay	
5.2. Sealing ability test	26

5.3.	<i>In vivo</i> biocompatibility (Sub-cutaneous tissue implantation test)	27
5.4.	Lithium ions levels in rat blood serum	28
6.	Statistical analysis	29
<u>Chapter III</u>	<u>Results</u>	
1.	Pulp capping experiments:	
1.1.	Micro-computed tomography and hematoxylin and eosin staining	30
1.2.	Masson tri-chrome staining	30
2.	In vitro studies:	
2.1.	Mechanical properties:	31
2.1.1.	Compressive and shear bonding strength	31
2.1.2.	Measurement of the released ions	32
2.2.	Cell studies:	32
2.2.1.	Proliferation assay	32
2.2.2.	Cytotoxicity assay	32
2.2.3.	Cell migration (wound healing assay)	32
2.2.4.	Alkaline phosphatase staining	33
2.2.5.	Alizarin red staining	33

3. Fluorescent immunohistochemistry staining	33
4. Comparative study results	34
4.1. Hydroxy-apatite formation	34
4.2. Sealing ability test	35
4.3. In vivo biocompatibility test	35
4.4. Lithium levels in the serum	36

Chapter IV Discussion

1. Discussion	37
2. Conclusions	49
3. References	50
4. Funds and grants	66
5. Published article	67
6. Academic presentations	70

Chapter V Figure and tables

1. Figures	71
2. Tables	88

Abbreviations

- **S-PRG:** Surface Pre Reacted Glass
- **LiCl:** Lithium Chloride
- **MTA:** Mineral Trioxide Aggregate
- **FDA:** Food and Drug Administration
- **ICP-AES:** Inductively Coupled Plasma-Atomic Emission Spectroscopy
- **HDPPCs:** Human Dental Pulp Stem Cells.
- **GIC:** Glass Ionomer Cement.
- **DW:** Distilled Water.
- **PFA:** Para-Form-Aldehyde.
- **LDH:** Lactate Dehydrogenase.
- **ALP:** Alkaline Phosphatase.
- **CPC:** Calcium Phosphate Cement
- **Li₂CO₃:** Lithium Carbonate.
- **β-TCP:** β-Tri-Calcium Phosphate
- **Ca(OH)₂:** Calcium Hydroxide
- **SBF:** Simulated Body Fluid
- **PTFE:** Polytetrafluoroethylene

Abstract

Surface pre-reacted glass (S-PRG) fillers are new bioactive materials used in dental clinical work to fill tooth defects. These fillers release various types of ions (Al^{+3} , BO^{-3} , Na^+ , SiO_3^{-2} , Sr^{+2} and F^-) and exhibit high biocompatibility, antibacterial capability, reduced plaque accumulation, and enhanced osteoblast differentiation. Our previous study has shown that the cement of S-PRG fillers could induce tertiary dentin formation in rat pulp capping models. Previous work has also shown that lithium ions can activate the Wnt/ β -catenin signaling pathway *in vitro* and induce dentin formation in pulpotomized teeth *in vivo*. In the current study, we sought to enhance the effect of the S-PRG cement by incorporating LiCl. The treatment of human dental pulp stem cells with eluates from the S-PRG/LiCl combination cements led to an upregulation in cell migration, differentiation, and mineralization *in vitro*. During pulp capping animal trials, S-PRG/LiCl cements could induce tertiary dentin formation 28-days post-capping. At 7 days post-capping, we identified both β -catenin expression and Axin2 expression using fluorescent immunohistochemistry, which is indicative of Wnt/ β -catenin signaling activity. Our study compared the novel combination to the mineral tri-oxide aggregate to reveal biocompatibility in subcutaneous tissues and *in vitro* capability of apatite formation with a better sealing ability of the S-PRG-containing cements. In conclusion, the S-PRG/LiCl cement was highly effective in the promotion of human dental pulp stem cell profiles and in the enhancement of reparative dentin formation in rat teeth through activation of the Wnt/ β -catenin canonical signaling pathway.

Chapter I

Introduction

The main goal of direct pulp capping is to preserve the vitality of pulp tissue, even when it is exposed to bacterial invasion, iatrogenic mechanical preparation, or trauma [1]. Calcium hydroxide has been used for over 60 years because it can induce reparative dentin formation [2, 3]. Calcium hydroxide can release hydroxyl and calcium ions, which create an alkaline bactericidal environment of the pulp tissues and which form necrotic tissue beneath the exposed pulp. Further, this inflammatory reaction may lead to increased cell differentiation, collagen secretion, and dentin formation [4, 5]. However, due to lower rates of clinical success that have been reported for the use of calcium hydroxide [6], the use of mineral trioxide aggregate (MTA) has aroused clinical interest [7]. MTA has been considered as a potential gold standard of vital pulp therapy because it showed higher integrity to the pulp tissues as compared to the use of calcium hydroxide [8], and revealed better success rates in clinical trials when used in various conditions, as compared to the use of other capping agents [7, 9, 10]. The exact mechanism of MTA's induction of dentin regeneration is unclear, but it may also release calcium ions that may show alkalinity to a level less than the level shown by calcium hydroxide, and can stimulate growth factor secretion to aid in migration, differentiation, and mineralized tissue formation [11, 12]. Many reports have demonstrated that MTA is bioactive even outside living cells. An *in vitro* study by Hosseinzade et al. showed that MTA could form hydroxyapatite on

the surface when immersed for 7 days in simulated body fluid (SBF), which was a solution developed by Kokubo in 1990 [13], and which contains multiple different ions (Na^+ , K^+ , Mg^{2+} , Ca^{2+} , Cl^- , HCO_3^- , HPO_4^{2-} , SO_4^{2-}) that are similar to the ionic composition of blood plasma [14]. MTA also showed high biocompatibility when implanted in rat dorsal subcutaneous tissue as compared to the biocompatibility shown by epoxy resin canal sealer (AH Plus, Dentsply Sirona, York, PA, USA), but had a similar effect to iRoot SP (Calcium silicate canal sealer, Innovative Bioceramics, Vancouver, Canada) [15, 16]. Although MTA bears some disadvantages (e.g., long setting time, does not bond with dentin, causes tooth discoloration, displays toxicity when freshly mixed, and is difficult to handle) [17, 18], its utility and benefits have inspired the dental research community and collaborators to invent new bioactive particles with high reliability. Indeed, various bioactive materials have been introduced and tested for their efficacy in dentin regeneration and pulpal healing, such as calcium-silicate-based cement, tetra-calcium phosphate cement, and “giomers” [19-22]. Giomer refers to any product that contains surface pre-reacted glass (S-PRG) filler particles: such as, stable glass ionomers formed by acid-base reactions of fluoro-boro-alumino-silicate glass with poly-alkenoic acid in a hydrated environment. The reaction occurs when silicate glass-treated surfaces react partially with a poly acrylic acid solution [23, 24]. Unlike other silicate materials that only release calcium ions, these tri-laminar structures of S-PRG fillers are able to release fluoride ions as well as five other ions (Al^{+3} , BO^{-3} , Na^+ , SiO_3^{-2} , and Sr^{+2}) [25]. They possess antibacterial properties [26-28]; can remineralize dentin, because of the fluoride and silicate ion content [29-31]; have acid-

buffering capacity [22, 32]; and can prevent plaque accumulation [24, 33]. The strontium and borate ions in these fillers are reported to have important roles in osteoblast differentiation and bone regeneration [34, 35]. These properties increase their importance and utility in the clinical preventive and operative dental fields [22, 36].

Our previous study demonstrated that a prototype pulp-capping cement that contained S-PRG fillers without additives such as lithium could induce reparative dentin formation in a rat model [37]. Lithium compounds were first introduced in clinical practice in 1970, after being approved by the FDA to treat acute symptoms of patients with bipolar diseases [38-40]. Subsequent *in vitro* studies have reported that lithium ions could accelerate bone regeneration and upregulate osteoblast differentiation and mineralization [41-43]. Ishimoto *et al.* revealed that 10 mM of LiCl can induce tertiary tubular dentin formation when applied topically to pulpotomized teeth in rats, and showed potential activation of the canonical Wnt/ β -catenin pathway when pulp cells were treated with lithium ions alone *in vitro* [44]. The Wnt/ β -catenin signaling pathway is activated in numerous biological cell functions and during organogenesis in the developing embryo [45-48]. Lithium ions trigger these signals through inhibition of the β -catenin destruction complex [41, 49, 50]. Han *et al.* reported that the inhibition of β -catenin expression decreased Runx2 expression and disrupted the differentiation of odontoblast cells in β -catenin-knocked-down rats. However, treating the cells with LiCl led to increased β -catenin accumulation and induction of the differentiation of dental pulp cells through Runx2 expression, that may play a role in odontoblastic differentiation and dentin secretion [51]. Since

β -catenin is involved in Wnt signaling transduction, Axin2 is known to inhibit this pathway through a negative feedback mechanism [52, 53]. Recent studies have reported that the temporary amplification of Wnt signals can maintain reparative dentin formation and preserve tooth vitality [48, 50, 54].

The other part of the study was to comparatively explore of the properties of the new lithium and S-PRG combination, and comparison of such properties to those of the current standard direct pulp capping material that is used in clinical cases (MTA). As mentioned previously, MTA can induce apatite formation *in vitro* [14,55]. To determine this capability of S-PRG-containing cements, we conducted *in vitro* trials using S-PRG and S-PRG/Li-100 mM. To evaluate the compatibility of the new S-PRG-containing cement, we performed a subcutaneous implantation test. Another important requirement for the pulp capping material is marginal sealing ability to prevent micro-leakage and secondary infection. To explore this property, a sealing ability test was performed using Rhodamine-B dye, and the penetration depth in bovine teeth samples was measured.

However, there is no study which demonstrates the involvement of Wnt signaling activation using lithium ions in dental pulp tissues *in vivo*. To our knowledge, this study is the first to demonstrate that the Wnt/ β -catenin signaling pathway directs activation in the pulp *in vivo* using a novel direct pulp capping cement that is combined with lithium ions and giomers.

2. Hypothesis of the study:

We hypothesized that incorporation of lithium ions into S-PRG fillers enhances reparative dentin formation through the activation of the Wnt/ β -catenin signaling pathway.

3. Objectives:

General objective of the study:

The general objective was to develop a new bioactive pulp capping cement using lithium-containing S-PRG fillers.

Specific objectives:

- 1.** To evaluate the lithium-containing S-PRG fillers as a direct pulp capping material in animal models using microcomputed tomography and histopathology methods.
- 2.** To determine the ideal concentration of LiCl that will be incorporated into S-PRG fillers to induce tertiary dentin regeneration.
- 3.** To examine the effect of the new lithium-containing cement on the Wnt/ β -catenin signaling pathway.
- 4.** To compare the new direct pulp capping cement with mineral tri-oxide aggregates in terms of biocompatibility, capability of marginal sealing, and ability to form hydroxyapatite *in vitro*.

4. Significance of the study:

This is the first study to characterize the S-PRG fillers containing lithium ions, on human dental pulp cells. Our study showed that this new lithium combination cement promoted cell functions by activating the endogenous Wnt/ β -catenin signaling pathway in the pulp tissue in rat models. Since this novel bioactive cement is potentially a promising material for clinical pulp regenerative therapy, human trials should be performed in near future.

5. Conflict of Interest:

The authors declare no conflict of interest in regard to this work.

Chapter II

Materials and methods

1. Materials

S-PRG powder and liquids with different LiCl contents were provided by Shofu Inc. (Kyoto, Japan) and the contents of each cement have been shown in Table 1. LiCl in powder form (Purity >98%, Nacalai Tesque, Kyoto, Japan) was added into the S-PRG liquid. Preparation was done by mixing the S-PRG filler with a copolymer of acrylic and tricarboxylic acid solution that contained LiCl in different concentrations to acquire the different cements. The powder and liquid parts were mixed on a paper pad for 40 seconds at a ratio of 1.5/1.0 wt (P/L). The time needed to complete the setting was 90 seconds. Mineral tri-oxide aggregate (Pro-Root MTA, Dentsply Sirona, Charlotte, NC, USA) was prepared using manufacturer's instructions, including mixing with distilled water, and has been used as a control for the pulp-capping experiment, and S-PRG without lithium content has also been used as a control in the *in vitro* studies.

2. Methods:

2.1. Animal experiments:

This study was conducted following approval from the Animal Care and Use Committee at Osaka University Graduate School of Dentistry (approval No. 28-013-0) in accordance with the ISO 7405 standard for evaluation of the biocompatibility of medical devices. Fifty-four 8-week-old male Wistar rats (180-200 g) (Japan Animal Inc., Tokyo, Japan) were used during the study. The rats were subdivided into groups according to the purpose of the experiment and for a period of cultivation, which has been described as follows.

2.1.1. Direct pulp capping procedure:

Forty-six rats were used for the direct pulp capping experiments. General anesthesia and local anesthesia were administered and pulp was exposed, under sterile conditions using medetomidine hydrochloride (Domitol; Meiji Seika Pharma Co., Ltd., Tokyo, Japan) at a dose of 0.3 mg/kg, midazolam (Dormicum; Astellas Pharma Inc., Tokyo, Japan) at a dose of 4.0 mg/kg, and butorphanol (Vetorphale; Meiji Seika Pharma Co., Ltd.) at a dose of 5.0 mg/kg. Then, local infiltrative anesthesia was given via a 0.5-mL injection of 2% lidocaine with 1:80,000 epinephrine (Xylocaine; Dentsply Sirona, Charlotte, NC, USA) [38]. The direct pulp capping procedure was performed on the bilateral maxillary first molars of each rat and drilled. A bowl-shaped cavity was prepared in the mesial pit of the occlusal surface using a steel round bur of 0.5 mm in diameter (Dentsply Sirona, Charlotte, NC, USA) with

pulp exposure smaller than 0.2 mm in diameter using low speed engine (VIVAMATE G5, NSK, Tochigi, Japan). The injured site was directly capped with the experimental cement using a sterile dental explorer tip (Hu-Friedy, Chicago, IL, USA). Then, the cavity was sealed with the glass ionomer cement (GIC, Fuji IX GP, GC, Tokyo, Japan) to prevent microbial leakage (Fig. 1a).

2.1.2. Micro-computed tomography and histopathological evaluation

The rats were sacrificed through the perfusion fixation method at different time points (1 day, 5 days, 7 days, 14 days and 28 days) post-operatively. Rats were intraperitoneally anesthetized, as previously described [56]. The operation was proceeded when the rats became unresponsive to the noxious stimuli. After perfusion with 4% paraformaldehyde (PFA, Nacalai Tesque), maxillae were dissected and the experimental teeth were collected and prepared for evaluation using a micro-CT scanner (R-MCT2, Rigaku, Tokyo, Japan). The new tertiary dentin structure was evaluated using TRI-3D BON software (Ratoc System Engineering, Tokyo, Japan). Extracted teeth were additionally fixed with the same fixative overnight. Specimens were decalcified in Kalkitox solution (Fujifilm Wako Pure Chemical, Tokyo, Japan) containing ethylene-diamine-tetra-acetic acid disodium salt (EDTA-2Na, 0.1 wt%) and hydrochloric acid solution (HCl, 4.8 wt%) and stored at 4°C for two nights. Then, specimens underwent dehydration in degraded concentrations of ethanol, which had been embedded in paraffin for histopathological sectioning with 5 µm thickness. Five different experimental groups (S-PRG, S-PRG/Li-10, S-PRG/Li-100, S-PRG/Li-1000 mM and MTA)

on day-28 have been prepared for histopathological assessment, using Myer's hematoxylin and eosin staining (Muto Pure Chemicals, Tokyo, Japan) to assess the formation of the new tertiary dentin bridges (n=5 for each group). Representative images were taken and observation of the dentin bridge formation was performed using a light microscope (Eclipse TS100, Nikon, Tokyo, Japan).

2.1.3. Masson tri-chrome staining:

The paraffinized block specimens that were prepared 5-, 7- and 14-days post-capping, were processed and stained using a Masson tri-chrome stain to assess the vascularity beneath the exposure site of the pulp tissue. Specimens were prepared the same as they had been in a previous process of deparaffinization and dehydration. Then, all sections were incubated sequentially in different developing solutions, starting with picric acid first in mordant solution, followed by Weighert's hematoxylin (Muto Pure Chemicals), bieberich scarlet acid solution (Masson B, Muto Pure Chemicals), phosphotungstic acid solution (Muto Pure Chemicals), and aniline blue solutions (Muto Pure Chemicals). Washing with citric acid (Muto Pure Chemicals) was completed between each step to give sharper staining. Following the mounting of the samples, light microscopic images were collected by a digital microscope (BZX-800, Keyence; Osaka, Japan). Three random sections from each sample were selected, and blood vessels were counted beneath the mesial exposure site along the mesial canal (n=3 for each group).

3. *In Vitro* studies

3.1. Mechanical Properties

3.1.1. Compressive and shear bond strength to dentin

Compressive strength tests for different S-PRG cements were conducted in accordance with ISO9917-1. Cylindrical specimens (dimension is 8:4 mm in length:diameter) were placed in a cabinet maintained at 37°C and a relative humidity of 100% for 1 h to complete the initial setting. Then, compressive strength was measured using a universal testing machine (Instron 5567, Norwood, MA, USA) at a crosshead speed of 1.0 mm/min. Shear bond strength to bovine dentin was measured using cylindrical samples of the cements after immersion in water for 24-h using a universal testing machine (Instron 5967) [37] (n=5).

3.1.2. Preparation of eluates and measurements of released ions

Four S-PRG cements (Table 1) were prepared, as described previously. The mixture was poured into a silicon ring mold (Diameter: 12 mm, Thickness: 1 mm) [37]. Then, the specimen was pressed between two slide glasses and incubated at 37°C in 100% relative humid environment for 15 min. Each cement disk was soaked in 5 mL of distilled water (37°C) for 7 days. The extract solutions have been filtrated with a filter of a pore size of 0.45 µm (Corning, New York, NY, USA). The concentrations of released ions (Al^{+3} , BO^{-3} , Na^{+} , SiO_3^{-2} or Sr^{+2}) were quantified using an induced coupled plasma spectrometry (ICP-8000, Shimadzu, Kyoto, Japan) using 1 mL of the extract (n=3). Due to the sensitivity of the fluoride ions, their

concentrations were measured using a pH/ISE meter (ORION-DUAL STAR, Thermo Fisher Scientific; Waltham, MA, USA) [57]. Before measurement of fluoride ions, the test solution was treated by the addition of 0.1 mL of the total ionic strength adjustment buffer (TISAB III, Thermo Fisher Scientific) per 1 mL of the test solution (n=3).

3.2. Cell studies

In vitro cell studies were conducted to clarify the optimal concentration of LiCl using the commercial human dental pulp stem cells (hDPSCs; Lonza, Basel, Switzerland). These cells were cultured in α -Minimum Essential Media (α -MEM, Gibco, Thermo Fisher Scientific) containing 10% fetal bovine serum (FBS; Gibco). Cells between passage 3 and passage 5 were used in subsequent assays.

3.2.1. Viable cell counting using trypan blue staining

hDPSCs were seeded at a density of 2×10^5 cells in 60-mm culture dishes with 3 mL α -MEM containing 1% FBS with or without eluates from S-PRG/LiCl (0 mM, 10 mM, 100 mM or 1000 mM) samples with an eluates-to-media ratio of 1:10. Eluates from the S-PRG cement without lithium content were used as controls. After 5 days, the cells were detached and stained with 0.4% trypan blue dye solution (Sigma-Aldrich, St. Louis, MO, USA). Viable bright cells were counted manually using a hemocytometer (Neubauer, Erma; Tokyo, Japan) (n=3).

3.2.2. Cytotoxicity assay

According to the ISO 10993-5 for the biological evaluation of medical devices and a slightly modified version of the cellular biocompatibility test, Lactate Dehydrogenase Enzyme kit (Takara Bio, Kyoto, Japan) was used to complete the enzymatic metabolic assessment of specimens on hDPSCs by measuring the lactate dehydrogenase activity to evaluate cytotoxicity. hDPSCs (2×10^5) were seeded into 60-mm dishes containing 3 mL of α -MEM with 10% FBS. After becoming confluent, the eluates from the four S-PRG groups (with an eluates-to-media ratio of 1:10) were separately added to 3 mL of α -MEM containing 1% FBS, and the media was changed into this and remained incubated for 24 h. The incubated solution (2 mL) was centrifuged at 2000 rpm for 5 min. Then, 100 μ L of the cell supernatant was reacted with 100 μ L of the lactate dehydrogenase (LDH) mixture (catalyst and dye from the kit) and incubated for 30 min. LDH is a eukaryotic enzyme that is released from damaged or lysed cells into the media. Measuring the amount of the released enzyme reflects the number of dead cells. LDH activity measured the absorbance of the red formazan that formed by the conversion of the lactate into pyruvate through the LDH enzyme. The absorbance was measured at 490 nm (Perkin Elmer, ARVO MX, Waltham, MA, USA) (n=3).

3.2.3. Cell migration (wound healing assay)

Cell migration was evaluated using a wound healing assay. Four-well silicon culture-inserts (Ibidi, Bavaria, Germany) were placed into 60 mm plates to create a 500- μ m horizontal gap.

hDPSCs, at a density of 5.5×10^3 , were seeded into the insert wells in 70 μ L media containing 10% FBS and incubated for 48 h. The inserts were then removed, and media were shifted into α -MEM containing 1% FBS and eluates. The plates were incubated for a further 48 h (Fig. 1b). Microscopic images (Eclipse TS100) were taken and the gap areas that had been covered by the migrated cells were analyzed by Image J software (NIH; Bethesda, MD, USA) (n=3).

3.2.4. Alkaline phosphatase staining

hDPSCs were cultivated at 5×10^4 cells/well in 24-well plates in α -MEM with 10% FBS. Monolayer cells were treated with the four different S-PRG eluates diluted with osteogenic differentiation-inductive media (α -MEM supplemented with 10% FBS, 10 mM β -glycerophosphate, 50 μ g/mL ascorbic acid, and 1 μ L/mL dexamethasone) for 2 weeks [58], whereby the media was changed every 3 days. The cells were fixed with a formalin neutral buffer solution with 3.7% of formaldehyde content (Kishida Chemical Co., Osaka, Japan), washed with PBS, and evaluated using an alkaline phosphatase (ALP) staining kit (Cosmo Bio Co. Ltd., Tokyo, Japan). Microscopic images of the stained wells were analyzed using image J (n=3).

3.2.5. Alizarin Red staining

hDPSCs were seeded at 1×10^5 cells/well in 12-well plates. After reaching confluence, the media were replaced by the differentiation-inductive media, along with the eluates from the four S-PRG specimens. Media had been changed every 3 days. Three weeks later [59], the cells

were fixed and stained using alizarin red solution (PG Research, Tokyo, Japan). The mineralized nodule that had been formed was dissolved with formic acid solution. Then, absorbance of the dissolved nodule was measured at 405 nm (ARVO MX) (n=3).

4. Assessment of the activation of Wnt/ β -Catenin signaling pathway

4.1. Fluorescent immunohistochemistry staining

For immunofluorescence staining, we used day-7 and day-14 prepared sections of the S-PRG and S-PRG/LiCl-100 mM cements, and they were compared to the intact tooth samples as controls for this experiment. They were evaluated using immunofluorescence staining to determine the activation of Wnt/ β -catenin signaling. Samples were deparaffinized, rehydrated, and washed with PBS. Trypsin from porcine pancreas (1 mg, Sigma-Aldrich, St. Louis, Missouri, USA) and Triton X-100 solution (Nacalai Tesque) were used consecutively for blocking non-specific reactions and permeabilization. The samples were incubated for 40 min at 4°C with rabbit monoclonal β -catenin (ab32572, Abcam; Cambridge, UK) or rabbit polyclonal Axin-2 (ab32197, Abcam). Samples were then washed and stained with goat anti-rabbit IgG (H+L) (Alexa Fluor 488, ab150077, Abcam). Nuclei were counterstained with Hoechst 33342 (Invitrogen; Waltham, MA, USA) and mounted using Vectashield (Vector Laboratories; Burlingame, UK). Images were taken using a digital microscope (BZX-800). Three random histological sections from each group were selected, and positive staining was observed using the BZX-800 view Analyzer Software (Keyence) (n=3 for each group).

5. Comparative study for various properties of lithium contained S-PRG

fillers:

5.1. Disk preparation:

The S-PRG cement and MTA disks were prepared using a mold with dimensions of 3 mm in diameter and 1 mm in thickness. Materials were mixed and poured into molds until complete setting (2 min for S-PRG cements and 5 h for MTA). Disks were sterilized by ethylene oxide gas (EOG) before use (n=3).

5.1.1. Hydroxyapatite formation:

Hydroxyapatite formation on the surface of the different cement disks were evaluated after soaking procedure in simulated body fluid (SBF) for 7 days or 14 days. SBF solution was prepared as described by Kokubo et al. [13] (Table 4). Following incubation for 7 days or 14 days, the specimens were placed in a dry keeper overnight (Sanplatec, Osaka, Japan), then coated with gold (Quorum SC7620, East Sussex, UK). Hydroxyapatite formation was observed using a scanning electron microscope (JSM-6390LV, JEOL, Tokyo, Japan).

5.2. Sealing ability test:

To assess the sealing ability of the experimental cement, twelve freshly extracted bovine incisors were ultrasonically cleaned to remove periodontal ligaments and were polished using a cup brush with polishing paste (Merssage, SHOFU, Kyoto, Japan). The crown part and 2 mm

of the apical part was removed under an irrigated high-speed hand piece and a needle-shaped diamond bur. Pulp tissue was extracted and canals were prepared 1 mm from the original diameter using the RaCe rotary system for canal preparation (FKG, Chaux-de-Fonds, Switzerland). Canals were cleaned using 2.5% NaOCl and 3% EDTA (Smear clean, Nishika, Shimonoseki, Japan). The roots were divided into two parts (each 8 mm in vertical length). Then, the twenty-four prepared canals were subdivided into three groups (8 prepared canals in each group) and the root was filled with one of the different experimental cement types (S-PRG, S-PRG/Li-100 mM, or MTA). The entire specimen was covered with nail varnish to prevent penetration of the dye through accessory canals or other parts, which meant that only the top surface remained opened. The specimens were immersed in DW for 12 h, then shifted to 0.1% rhodamine-B dye for 24 h at room temperature. The rhodamine-B solution was prepared by dissolving 1.31 g of rhodamine-B powder (> 95% purity, Sigma Aldrich) into 100 mL of DW. The samples were washed and cleaned under running tap water to remove the excess dye and cut using a diamond blade (Buehler IsoMet, Lake Bluff, Illinois-IL, USA) longitudinally into two sections. Dye penetration was evaluated by imaging the samples under a stereomicroscope (SMZ-U, Nikon SM, Tokyo, Japan). The penetration depth of the rhodamine-B dye was evaluated in pixels using viewer-measuring tools (SMZ-U, Nikon SM).

5.3. *In vivo* biocompatibility (Sub-cutaneous tissue implantation test):

Animal studies were conducted under the approval of the Institutional Animal Care and Use Committee of Osaka University Graduate School of Dentistry (approval No.29-028-0). Sterile

polytetrafluoroethylene (PTFE) tubes (inner diameters at 1.5 mm and 6 mm in length) were filled with S-PRG, SPRG/LiCl-100 mM, or MTA, and empty tubes were prepared. The experiment was conducted on eight-8 weeks-old male Wistar rats. The hairs on the dorsum of the rats were shaved and disinfected with 5% iodine before the operation. Disposable scalpel (Kai Medical, Tokyo, Japan) was used to make 4 subcutaneous incisions (2 cm in length) at the lateral sides of the rat's dorsum. Four PTFE tubes containing the different materials were implanted. An empty tube was used as a control group. The incisions were sutured using a sterile 7-0 polypropylene monofilament suture and a multi-pass reverse cutting needle (Ethicon, Johnson and Johnson, Somerville, New Jersey, USA).

One week or two weeks following the operation, tubes with the surrounded tissue were collected after sacrificing. Tissues were fixed using 4% paraformaldehyde (PFA, Nacalai Tesque) for two nights. Inflammatory reaction was evaluated using the hematoxylin and eosin staining method. Images were taken using a digital microscope (BZX-800) and manual counting for inflammatory cells was performed (n=3).

5.4. Lithium ion levels in rat blood serum

The pulp capping experiment was completed, as previously described, in the remaining nine rats. 1-, 3-, and 7-days post-operatively, 5 mL of blood samples were collected intracardially to evaluate the concentration of lithium ions in the serum using the method of the flame atomic absorption spectroscopy (SpectrAA-240, Agilent Technologies; Santa Clara, CA, USA) (n=3).

6. Statistical methods

Numerical values of all experimental groups were statistically evaluated using a one-way ANOVA with the Tukey–Kramer post hoc tests for cell studies and the Student's *t*-test for the mechanical properties assessment. The tests used were processed by StatView-J 5.0 (SAS Institute Inc. Cary, NC, USA). P-values less than 0.05 were considered statistically significant.

Chapter III

Results

1. Pulp capping experiments

1.1. Micro-computed tomography and hematoxylin and eosin staining

Figure 2a-2e shows the micro-CT images of the maxillary first molars 28 days after direct pulp capping with the five different materials, as processed with the TRI-3D BON software. The light blue regions indicated the tertiary (reparative) dentin structures. Figure 2f-2o shows the H&E-stained samples at lower (Fig. 2f-2j) and higher (Fig. 2k-2o) magnification to show the tertiary dentin bridge formation beneath the cavity prepared sites. Treatment with S-PRG/LiCl-10 mM and S-PRG/LiCl-100 mM led to the formation of complete tertiary dentin structures that were continuous with the primary dentin (PD) and devoid of defects, similar to those which had been produced by MTA, and which were used as positive controls (Fig. 2k, 2l and 2o). In contrast, S-PRG/LiCl-1000 mM treatment led to incomplete tertiary dentin formation (Fig. 2c, 2h and 2m) and the S-PRG cement without lithium ions also resulted in a defected tertiary dentin structure (Fig. 2d, 2i and 2n).

1.2. Masson tri-chrome staining results:

Masson tri-chrome staining was conducted to assess the vascularity beneath the injury site. S-PRG groups were compared to the control group (intact tooth), and displayed some dilated blood vessels beneath the exposure 5 days postoperatively. Further, the groups showed a

comparable tendency for the number of dilated blood vessels (Fig. 3a-3c and 3m), except for S-PRG/Li-1000 mM, which showed a higher number of blood vessels, indicating severe hyperemia (Fig. 3d). Day-7 and 14 samples showed a decrease in the number of dilated blood vessels, compared to the samples at day-5. Comparing day-5 and day-14, a statistical difference was observed in S-PRG/Li-100 mM (Fig. 3c, 3h, and 3n). Further, comparing day-7 and day-14 to day-5 also revealed a significant decrease in S-PRG/Li-1000 mM, as shown in Fig. 3n ($p < 0.05$).

2. *In vitro* studies

2.1. Mechanical properties

2.1.1. Compressive and shear bonding strength

Table 2 describes the physical properties of the experimental cements. We found a tendency for decreased compressive strength of the experimental cement samples with increasing lithium concentrations. S-PRG/Li-100 mM and S-PRG/Li-1000 mM specimens showed significantly decreased compressive strength compared to controls ($p < 0.05$). However, there was no significant difference in the shear bond strength of the cements to dentin among any of the groups ($p > 0.05$). The failure mode of the shear bond strength test using S-PRG and S-PRG/LiCl was an interface failure among all the specimens.

2.1.2. Measurement of the released ions

The values of the various ions leached from the different S-PRG cements are shown in Table

3. The amount of lithium ions released from S-PRG/Li-10, S-PRG/Li-100, and S-PRG/Li - 1000 mM were 0.1 mmol/L, 1.9 mmol/L, and 21.5 mmol/L, respectively.

2.2. Cell studies

2.2.1. Proliferation assay

hDPSC survival was maintained in the presence of the eluates from S-PRG/LiCl-10 mM and S-PRG/LiCl-100 mM samples, with no significant difference, as compared to that in the presence of eluates from the no-lithium containing control specimens ($p>0.05$). However, eluates from the S-PRG/LiCl-1000 mM group showed significant inhibition of hDPSC growth ($p<0.05$) (Fig. 4a).

2.2.2. Cytotoxicity assay

The amount of the LDH enzyme from the cells exposed to S-PRG/LiCl-10 mM and S-PRG/LiCl-100 mM were not significantly different from the amount expressed by cells exposed to control (no lithium) eluates ($p>0.05$). In contrast, cells exposed to S-PRG/LiCl-1000 mM showed higher cytotoxicity as compared to the other specimens, including the control group ($p<0.05$) (Fig. 4b).

2.2.3. Cell migration (wound healing assay)

Significantly higher cell migration was observed in the cultures exposed to all the lithium-containing eluates, as compared to those exposed to the control eluates ($p<0.05$). However, S-PRG/LiCl-100 mM showed the greatest effect on cell migration, as compared to the other lithium-containing groups (Fig. 4c).

2.2.4. Alkaline phosphatase staining

The intensity of ALP staining was significantly higher in cells that were cultured in the presence of eluates from the S-PRG/LiCl-100 mM group, but declined significantly in the S-PRG/LiCl-1000 mM group ($p<0.05$), as compared to controls (Fig. 4d).

2.2.5. Alizarin Red staining

For cells cultured in the presence of S-PRG/LiCl-100 mM eluates, there was a significant increase ($p<0.05$) in the absorbance of the dissolved mineralized nodule, as compared to the absorbance demonstrated by other groups (Fig. 4e).

3. Immunofluorescence staining

Expression of β -catenin was evaluated on the odontoblastic cell layer beneath the cavity preparation site (Fig. 5a). Fig. 5b-5p shows the immunofluorescence expression of β -catenin on the odontoblastic cell layer of the sections prepared 7- or 14-days post-capping. Treatment with S-PRG in the absence of lithium led to weak expression of β -catenin in the layer of the odontoblastic cells, similar to the expression pattern observed in the intact tooth (control) (Fig.

5b-5g). Comparatively, S-PRG/LiCl-100 mM-treated specimens led to strong expression levels of β -catenin in the odontoblastic cell layer, distributed in a localized pattern at day-7 (Fig. 5h-5j). In day-14 samples, a lower expression of β -catenin was observed with S-PRG/LiCl-100 mM treatment, similar to that of the control (Fig. 5n-5p) and S-PRG groups (Fig. 5k-5m). Higher magnification of the day-7 samples from the S-PRG/LiCl-100 mM group revealed β -catenin translocation to the nuclei of odontoblastic cells, as well as its expression in the cytoplasm (Fig. 5q-5s). Quantitated values of β -catenin expression indicated a significant increase in the expression of β -catenin in the S-PRG/LiCl-100 mM group ($p < 0.05$) at day-7 as compared to in other groups (Fig. 5t). The expression of Axin2 in the odontoblastic cell layer of the S-PRG group was similar to that of the intact control group at day-7 and day-14 (Fig. 6d-6f, 6j-6i). However, treatment with S-PRG/Li-100 mM led to strong expression of Axin2 in the odontoblastic cell layer at both time points (Fig. 6g-6i, 6m-6o). Axin2 expression in higher-magnification images showed a diffused pattern (Fig. 6p-6r). The quantitated values indicated no significant decrease in Axin2 expression in the S-PRG/Li-100 mM group from day-7 to day-14 (Fig. 6s).

4. Comparative studies results

4.1. Hydroxy-apatite formation:

SEM images showed the apatite that formed following 7- and 14-days of immersion in SBF. Irregular rounded apatite-like structures were observed on the surfaces of the MTA, S-PRG, and

S-PRG/Li-100 mM groups (Fig. 7a-7c) following 7-days of incubation. In the case of 14-days for the specimens, the already-formed irregular structures in each group coalesced, forming a layer of apatite on the surface of the disks (Fig. 7d-7f).

4.2. Sealing ability test

The bovine teeth canals that were sealed with S-PRG or S-PRG/Li-100 mM cements showed a lower rhodamine-B dye penetration depth of 82.8 pixels and 110.7 pixels, respectively (Fig. 8a-8d), compared to the MTA, which displayed deeper penetration of 365.4 pixels (Fig. 8e and 8f). Statistical analyses demonstrated a significant increase in rhodamine-B dye penetration in the MTA group compared to the S-PRG and S-PRG/Li-100 mM groups ($p<0.05$) (Fig. 8g).

4.3. *In vivo* biocompatibility test:

Stained subcutaneous tissue histological images were taken from the edges, facing the material of the tube. Empty tube samples represented the control group of this study. At day-7, all the study groups showed some inflammatory cells infiltration (black arrows), blood vessels (red asterisk), fibroblast cells (green arrows), and adipocytes (orange arrows). Infiltration of inflammatory cells demonstrated similar tendencies across all study groups (Fig. 9a-9h). However, S-PRG samples showed a statistically significant decrease compared to other groups ($p<0.05$). By day-14, all the experimental and control groups displayed inflammation regression. This regression was significant when compared to that of the day-7 samples. However, no

significant difference was observed in the number of inflammatory cells between the groups at day-14 (Fig. 9i).

4.4. Lithium levels in the serum

The concentration of lithium ions in the peripheral blood circulation was less than 0.01 mmol/L for the samples at 1 day, 3 days, and 7 days, after the topical application of S-PRG/LiCl-100 mM cement.

Chapter IV

Discussion

The current standard direct pulp capping material (MTA) works with a relatively higher success rate compared to the conventional calcium hydroxide [9, 10]. Despite this, it has some disadvantages, as mentioned in the introduction. An ideal direct pulp capping material must form hard dentinal tissues, regardless of easy handling and application. Researchers have been working diligently to provide such materials, but they have not achieved this aim.

S-PRG fillers have received more attention recently due to their distinctive properties, which include their ability to release multiple ions that may exert various biological effects [25]. S-PRG fillers are involved in many dental products that can be used as composite filling or varnish materials for clinical use, due to the following characteristics: their antibacterial effects, enamel remineralization abilities due to their release of fluoride ions [60, 61], and induction of hard-tissue formation and modulation of the healing process of tissues through modulating the expression of the SDF1 and TGF- β genes as reported by Okamoto et al. [62]. He also found that there is no significant difference in the proliferation rate of dental pulp cells when co-cultured with S-PRG or plain media [62].

In the current study, we attempted to enhance the efficacy of the S-PRG fillers as dental pulp-capping agents by incorporating lithium ions. This novel combination activated the Wnt/ β -catenin signaling pathway as a part of the healing process of the dentin-pulp complex *in vivo*.

The lithium combinations have been used in treating acute symptoms in patients with bipolar diseases since 1970 after being proved by the FDA [38, 63]. A previous clinical study using magnetic resonance imaging reported that lithium ions acted by increasing the volume of the hippocampus in euthymic elderly patients with bipolar disorder who received lithium treatment for more than 61 months [64]. Additionally, lithium also acts by preventing the loss of grey matter [65], which is a neuroprotective effect.

Recently, lithium was reported to be involved in bone regeneration because it acts by activating important signaling pathways, namely the Wnt/ β -catenin signaling pathway [41]. Many tailored studies were performed to assess the ideal concentration of lithium that may be effective to activate these signaling pathways and aid in tissue healing and regeneration. However, these ideal concentrations were different across conditions and were ultimately found to be dependent on the size of the injury and the type of the carrier [66-71].

In this study, the lithium ions enhanced dentin regeneration in rat models when they were incorporated into the S-PRG cement to be applied as a direct pulp capping cement. The pulp capping experiments resulted in complete tertiary dentin formation when the S-PRG fillers were combined with lower concentrations of LiCl. Although the S-PRG/Li-10 and S-PRG/Li-100 mM cements were similar to the dentin bridge formed by the one formed by MTA, the S-PRG/Li-1000 mM cement resulted in an incomplete bridge formation, while the S-PRG without lithium cement resulted in a defected structure (Fig. 2k-o).

Masson tri-chrome staining outcomes showed the presence of dilated blood vessels that were displayed in all samples of the day-5 groups. However, severe hyperemia was denoted by the S-PRG/Li-1000 mM cement of the day-5 samples, compared to other study groups (Fig. 3d). Although dilated vessels can indicate active dentinogenesis, it may also suggest a severe inflammatory reaction within the tissue that may interfere with the pulp healing and regeneration when the intensity of the stimulus increases, as reported by Yu et al. [72]. The statistics show a significant increase in the number of the dilated blood vessels in S-PRG/Li-1000 mM group (Fig. 3n). The hyperemia of S-PRG/Li-1000 mM was resolved to be the same as the control intact tooth group by day-7 and day-14. Blood vessels dilation is one of the important inflammatory response signs. Similar outcomes were denoted by Six et al. [73], whereby class V cavities were restored in rat models using FUJI IX glass ionomer cement (GIC). The histopathological results following 8 days post-operatively indicated a mild inflammatory reaction beneath the cavity preparation site that resolved by day-30. In the current study, we exposed the pulp, which made a direct contact between the pulp cells to the pulp capping cement. We suggest that this severe hyperemia may occur because of the released lithium ions chemically stimulate the cells to release cytokines and induce inflammatory responses at the early stages of healing. Lithium ions showed both reactions, with inducer and inhibitor effects on the dental pulp stem cells. Presently, the effect of lithium on inflammatory reactions is unclear, though some studies have shown that the inflammatory response to lithium is induced by the production of pro-inflammatory cytokines, including IL-4 and 6 [74, 75]. Nevertheless,

some other reviews demonstrated that lithium may exhibit anti-inflammatory effects due to the ability of lithium ions to suppress the expression of some inflammatory cytokines, e.g., COX-2, IL-1 β , and produce TNF- α as well as enhance the synthesis of IL-2 and IL-10 [75-77].

To assess the ideal concentration, *in vitro* studies were also performed to evaluate the behavior of hDPSCs following treatment with eluates of the experimental cements that bear different Li concentrations. Our study found that eluates from S-PRG/Li-100 mM samples could significantly enhance cell migration, differentiation, and mineralization with no toxicity to the dental pulp stem cells, as compared to the results observed in control group and other groups (Fig. 3b, 3d, and 3e, respectively). In contrast, S-PRG/Li-1000 mM was found to decrease cell profiles, with lower proliferation and expression of LDH, which is indicative of cell injury that is probably caused by the chemical-stimulated cells of the S-PRG/Li-1000 mM group, which showed higher lithium ion release capabilities (Fig. 3a and 3b, Table 3). This difference between the behavior of the cells cultured in S-PRG/Li-100 mM and S-PRG/Li-1000 mM could indicate that there is a borderline between compatible and toxic combinations to the cells.

These *in vitro* and Masson trichrome staining results may help to explain the tendency of tertiary dentin formation in previous pulp-capping experiments. Lili *et al.* reported that LiCl at 50 mM, 100 mM, and 200 mM doped into calcium phosphate cements (CPC) can accelerate bone regeneration in a model for osteoporosis *in vivo*. *In vitro*, they found that CPC/Li-50 and 100 mM induced osteoblastic cell differentiation and mineralization, but that higher

concentrations (CPC/Li-200 mM) inhibited these functions [41]. We similarly found an optimal dose of Li in hDPSCs cells based on our results.

The mechanical properties of the cements were also evaluated. No statistical differences were observed in the shear bond strength to the dentin after LiCl incorporation into the S-PRG fillers (Table 2). However, S-PRG/Li-100 mM and S-PRG/Li-1000 mM specimens had significantly decreased the compressive strength compared to the control. A similar tendency was reported by Vahabzadeh et al. [78], who noticed that there was a deterioration in the mechanical characteristics of β -Tri calcium phosphate cements when doped into higher concentrations of pure lithium oxides. They assumed that the lithium ions, which were small molecules, were replaced with other cationic molecules with larger sizes, such as Ca^{+2} . When such replacement occurs, it results in a disturbance of the net structure of the cement. Thus, we suggest that a similar phenomenon may occur and lead to weakening of the cement and subsequent release of more ions into the surrounding environment.

Lithium ions released from the different cement samples are directly proportional to the LiCl molarity incorporated into the cement, and the release of other components were similar among the specimens (Table 3). This suggests that the eluted lithium ions have a major influence on the behavior of the cells both *in vitro* and *in vivo* [41, 78].

The canonical Wnt/ β -catenin signaling pathway plays an important role in oral tissue formation during embryogenic development [48]. β -catenin accumulates in the cytoplasm of cells and then translocates into the nucleus to trigger the expression of different genes associated with

tooth development at various stages [62]. In the current study, LiCl-100 mM was shown to activate this signaling pathway. As suggested by Joje et al. [80], this may be achieved by inhibiting GSK-3 β molecules that deregulate the function of the β -catenin destruction complex and produce signals. Immunofluorescence-stained sections showed intense β -catenin expression in the odontoblastic cell layer in day-7 samples treated with S-PRG/Li-100 mM (Fig. 5h-5j). The magnified images further suggest translocation of β -catenin into the nuclei of these odontoblastic cells (Fig. 5q-5s), which is indicative of canonical signal activation. β -catenin expression in the S-PRG/Li-100 mM group declined at a later time point (Fig. 5n-5p), which is suggestive of a temporary activation of the Wnt/ β -catenin signaling pathway as part of the reparative process. The outcomes of this assay are in accordance with those of the study by Han and colleagues [51]. In their study, the authors reported that β -catenin activated Runx2 and enhanced odontoblastic differentiation when the tooth pulp was capped with MTA.

Axin2 is a target and negative regulator of the canonical pathway through β -catenin degradation [81]. In our study, Axin2 was highly expressed in the S-PRG/Li-100 mM pulp-capped groups at day-7 and day-14, as compared to the S-PRG cement without lithium or the intact teeth controls (Fig. 5a-5n). Axin2 expression was diffused within the odontoblastic cell layers (Fig. 5p-5r). This pattern of expression was similar to that described by Bernkopf et al. [58]. However, the reason for the continuous expression of Axin2 through day-7 to day-14 is unclear. Babb et al. previously reported that Axin2 had roles in β -catenin deregulation, which may or may not involve other signaling molecules [54]. A previous study found no increase in the

Wnt/ β -catenin signaling pathway in primary odontoblasts, but showed that the pathway was promoted during reparative dentin formation in response to pulpal damage. Another study by Jho *et al.* demonstrated that Axin2 act as a negative feedback loop regulator in Wnt/ β -catenin signaling, as it controlled signaling duration and intensity [81]. The hypothesis for the Axin2 expression is being investigated by researchers, but some explanations have been reported. Some hypothesize that Axin2 may be involved in another signaling pathway, such as the transforming growth factor β signaling pathway, as reported by Furuhashi *et al.* [82]. Other theories may explain the continuous expression of Axin2, as explained by a study by Leung *et al.* [83], who claimed that the Axin2 gene is a downstream target of the Wnt/ β -catenin signaling pathway. They concluded that the Axin2 genes can be activated through β -catenin binding to the T-cell factor protein (TCF) complex. As a result of this complex, Axin2 was robustly expressed in the cells. Our present findings can confirm their hypothesis; we found that β -catenin expression was significantly high during early stages and declined sharply later, while Axin2 showed continuous expression. Inhibition of β -catenin expression at day-14 may occur due to the negative regulatory effect of Axin2.

The other aim of the study was to compare the lithium combination (S-PRG/Li-100 mM) to that of the current standard pulp capping material, MTA. In terms of hydroxy-apatite formation, S-PRG, S-PRG/Li-100 mM, and MTA demonstrated apatite-like structure formation on the surface of the disk after soaking in simulated body fluid (SBF) at different time-points. SBF contents are similar to the body plasma components first described by

Kokubo et al. [13]. Following the incubation for 7 days, they demonstrated irregular structures under SEM observation (Fig. 7a-7c). Further, their immersion for two weeks resulted in irregularities in the coalescence to form an apatite-like layer (Fig. 7d-7f). Our current observations are in line with those of previous reports [14,84]. The mechanism of the apatite formation described by Niu et al. suggests that the apatite formation starts by hydrolysis and ion exchange, followed by calcium silicate hydrate formation, and their binding to calcium ions results in amorphous calcium precipitation, which leads to nucleation and is lastly transformed to carbonate apatite [84]. We hypothesized that a similar reaction may occur using S-PRG cement types. The S-PRG cements apatite formation may be different from that of the MTA because of different nucleating calcium silicate niches as compared to that of the MTA cement, which contains calcium as one of its abundant components [55], while the S-PRG cement did not contain calcium in its fillers. However, the SBF solution provided calcium ions to form the nucleation site, as it combines with rich silicate ions in the S-PRG structures to proceed with the carbonate apatite formation process [14].

Due to the importance of the sealing ability of the direct pulp capping cement in preventing micro-leakage and secondary coronal infection, sealing ability tests were conducted through immersion of bovine canals filled with different cement types in 0.1% rhodamine-B solution for 24 h. S-PRG and S-PRG/Li-100 mM showed imperfect sealing ability that was better than that of the MTA, with statistical significance in the differences in dye penetration (Fig. 8g).

The sealing ability of the S-PRG cement has been first reported in this study, as no previous studies have reported the sealing ability of giomers as a direct pulp capping cement. Another study reported similar inferior sealing properties using pro-root MTA [85]. They revealed that the addition of calcium chloride can decrease marginal leakage as compared to the results with conventional MTA types. However, Abimanyu et al. showed that MTA may have good sealing properties similar to biodentine, which is a tri-calcium silicate base cement that is similar to MTA in nature but distinguished by easier handling technique and faster setting time as compared to that with MTA, and is used for pulp capping or perforation repair [86]. We postulated that these differences in both studies are due to differences in the dye type and assessment methods. In the study by Abimanyu et al., methylene blue dye was used, whereas the current study was performed using rhodamine-B dye. Further, rhodamine-B dye has some advantages over methylene blue dye, in terms of its ability to diffuse into human dentin, which makes it more reliable as compared to methylene blue [87]. Moreover, rhodamine-B dye has smaller particle sizes similar to the size of bacterial toxins and can be easily detected, in contrast to methylene blue dye, which can be dissolved, and its maximum diffusion becomes difficult to observe [87].

To evaluate the biocompatibility of the three pulp capping materials, a subcutaneous tissue implantation test was conducted in rat models. The results showed that MTA and S-PRG/Li-100 mM groups showed some inflammatory cells in a way similar to that presented by the control group, which was implanted using empty PTFE tubes that had been implanted for 7

days. The S-PRG group demonstrated the least reaction as compared to that by the control group, MTA group, and S-PRG/Li-100 mM groups at day-7. We suggest this response occurred due to earlier recovery of the cells, in contact to S-PRG or the delayed reaction after day-7. The number of inflammatory cells decreased significantly in all experimental groups and control groups at day-14, indicating biocompatibility to the surrounding tissues that were in direct contact with the cement parts. A similar regression of inflammation was demonstrated by many researchers using MTA [16, 85]. The results of day-7 presented that the S-PRG cements were biocompatible to the subcutaneous tissues, and even after LiCl addition, they displayed biocompatibility that was similar to the results with MTA. These results are the first to demonstrate the behavior of S-PRG before addition and after addition of lithium. However, further studies using immunohistochemistry to mark the inflammatory cells and macrophages will be needed for detailed information.

For biosafety purposes, we measured the concentration of lithium ions in the serum of rats through blood draws taken 1 day, 3 days, and 7 days after topical application of the experimental cement. Our study found that the lithium ions released from the S-PRG/Li-100 mM sample into the peripheral circulation were nearly undetectable (<0.01 mmol/L). This level is lower than that described by Hanak et al. [59], who conducted tests to ascertain the level at which the administration of Li_2CO_3 by intraperitoneal injection caused acute poisoning. In their study, the lithium concentration in the plasma was higher than 1.0 mmol/L. Moreover, the renal lithium clearance, as described by Smith and Thomsen, was 0.20 ± 0.04 ml/min per 100 g of

body weight of healthy Wistar rats [88]. They received an intraperitoneal injection of 150 mM of LiCl for 2.5 h before the clearance test.

Despite lithium demonstrating a therapeutic effect [89], it also displayed various side effects due to prolonged utilization. Side effects range from mild symptoms, such as weakness, ataxia, tremor, diarrhea, and poor concentration to severe signs of toxicity, such as vomiting, slurred speech, confusion, gross tremor, and lethargy [90].

Our current results suggest the biosafety of S-PRG/LiCl-100 mM when used in a cement form topically applied for dental repair. Although results of *in vitro* assessment of lithium ions released showed higher concentrations of lithium in S-PRG/Li-100 mM (the therapeutic level that has been approved by the FDA (0.3 mmol/L – 1.3 mmol/L)) [38], this phenomenon has not occurred in our rat models. This may have happened due to the periodical clearance of lithium ions in animals, which involves excretion of the ions through the renal system, and technically implies that less ions will be leached into circulation. Moreover, small exposure sizes and amounts were used for topical application in the direct pulp capping experiment. This takes setting time into consideration as the cement needs approximately 90 seconds to set and only the surfaces facing the pulp are available to release the ions at the injury site.

Overall, the most effective lithium ion concentration in this study, LiCl-100 mM, contrasts with the findings of a previous study by Ishimoto's group, which showed a lower concentration, LiCl-10 mM, to be the most effective [44]. We posit that this variation may be due to the different carriers used in the two studies: S-PRG fillers versus hydrogel. While S-PRG acts as

a carrier that controls the amount of ions released, the hydrogel is a biodegradable carrier and can release the entire amount of the carried molecules.

This novel cement combining S-PRG fillers and LiCl-100 mM showed promising outcomes as an alternative pulp-capping agent that can activate the Wnt/ β -catenin signaling pathway, mimicking the biological processes of tissue healing. Additional benefits include that it could show decreased micro-leakage and antibacterial activity. However, this novel material requires further investigation for clinical translation in future.

4. Conclusions

In conclusion, this novel material may be ideal and more suitable for clinical implementation as a direct pulp-capping cement.

1. S-PRG/Li-100 mM promoted the migration, differentiation, and mineralization of hDPSCs *in vitro* with no cellular toxicity effect.
2. The new lithium combination proved its capability to induce reparative dentin formation in biomimicry approaches using rat pulp capping models.
3. The mechanism of tertiary dentin formation may be partly due to the activation of Wnt/ β -catenin canonical signaling *in vivo*.
4. S-PRG/Li-100 mM displayed better properties that act in a way similar to MTA or exceed in action with respect to micro-leakage prevention.
5. The biosafety of S-PRG/Li-100 mM has been verified, as it has been released in small amounts in the serum of rat models.

We encourage the research translation of using S-PRG/LiCl as a direct pulp capping cement in dental clinics by starting human clinical trials or using bigger animals.

3. References

- [1] D. Tziafasa, A.J. Smithb, H. Lesotc, Designing new treatment strategies in vital pulp therapy, *J Dent.* 28 (2) (1999) 77-92. (DOI: [https://doi.org/10.1016/S0300-5712\(99\)00047-0](https://doi.org/10.1016/S0300-5712(99)00047-0))
- [2] GT.-J. Huang, Dental pulp and dentin tissue engineering and regeneration: advancement and challenge, *Front Biosci (Elite Ed)* 3 (2011) 788-800. (PMCID: PMC3289134)
- [3] M.L.R. Accorinte, A.D. Loguercio, A. Reis, E. Carneiro, R.H.M. Grande, S.S. Murata, R. Holland, Response of human dental pulp with MTA and calcium hydroxide powder, *Oper Dent.* 33 (5) (2008) 488-495. (DOI: 10.2341/07-143).
- [4] A. Njeh, E. Uzunoğlu, H. Ardila-Osorio, S. Simon, A. Berdal, O. Kellermann, M. Goldberg, Reactionary and reparative dentin formation after pulp capping: Hydrogel vs. Dycal, *Evidence-Based Endodontics* 1:3 (2016) (DOI 10.1186/s41121-016-0003-9)
- [5] Y. Nishikawa, S. Matsuda, Y. Nakayasu, J. Toriya, Y. Yokoi, M. Shoumura, N. Okafuji, T. Kawakami, N. Osuga, Reactions of the dentin-pulp complex to calcium hydroxide paste in rats, *J. Hard Tissue Biol.*, 26[2] (2017) 169-176.
- [6] D. Sönmez, Ca(OH)₂ pulpotomy in primary teeth. Part I: internal resorption as a complication following pulpotomy, *Oral Surg. Oral Med. Oral Pathol. Oral Radiol.*, 106 (2) (2008) e94-e98.
- [7] T.J. Hilton, Keys to clinical success with pulp capping: A review of the literature, *Oper Dent.* 34 (5) (2009) 615–625. (DOI: 10.2341/09-132-0)

- [8] R.P. McNamara, M.A. Henry, W.G. Schindler, K.M. Hargreaves, Biocompatibility of accelerated mineral trioxide aggregate in a rat model, *J Endod.* 36 (11) (2010) 1851-1855. (DOI: 10.1016/j.joen.2010.08.021).
- [9] L. Awawdeh, A. Al-Qudah, H. Hamouri, R.J. Chakra, Outcomes of vital pulp therapy using mineral trioxide aggregate or biodentine: A prospective randomized clinical trial, *J Endod.* 44 (11) (2018) 1603-1609. (DOI: 10.1016/j.joen.2018.08.004)
- [10] N. M. Mostafa, S. A. Moussa, Mineral trioxide aggregate (MTA) vs calcium hydroxide in direct pulp capping – literature review, *On J Dent & Oral Health.* 1 (2) (2018) 1-6. (DOI: OJDOH.MS.ID.000508).
- [11] K. Peycheva, Pulp-capping with mineral trioxide aggregate, *Acta-Medica Bulgarica* 42 (2) (2015) 23-29 (DOI: <https://doi.org/10.1515/amb-2015-0014>)
- [12] T. Okiji, K. Yoshida, Reparative dentinogenesis induced by mineral trioxide aggregate: A review from the biological and physicochemical points of view, *Int. J. Dent* (2009) (DOI:10.1155/2009/464280).
- [13] T. Kokubo, H. Takadama, How useful is SBF in predicting in vivo bone bioactivity?, *Biomaterials* 27 (2006) 2907–2915. (DOI:10.1016/j.biomaterials.2006.01.017)
- [14] M. Hosseinzade, R. K. Soflou, A. Valian, H. Nojehdehian, Physicochemical properties of MTA, CEM, hydroxyapatite and nano hydroxyapatite-chitosan dental cements, *Biomed. Res.* 27 (2) (2016) 442-448.

- [15] W. Zhang and B. Peng, Tissue reactions after subcutaneous and intraosseous implantation of iRoot SP, MTA and AH Plus, *Dent Mater J.*, 34 (6) (2015) 774–780. (DOI: 10.4012/dmj.2014-271).
- [16] P. Karanth, M. K. Manjunath, Roshni, E. S. Kuriakose, Reaction of rat subcutaneous tissue to mineral trioxide aggregate and portland cement: A secondary level biocompatibility test, *J. Indian Soc. Pedod. Prev. Dent.*, 31 (12) (2013) 74-81. (DOI: 10.4103/0970-4388.115698).
- [17] C.P. Lucas, R. Viapiana, R. BossoMartelo, J.M. Guerreiro-Tanomaru, J. Camilleri, M. Tanomaru-Filho, Physicochemical Properties and Dentin Bond Strength of a Tri-calcium Silicate-Based Retrograde Material, *Braz. Dent. J.* 28 (1) (2017) 51-56. (DOI: 10.1590/0103-6440201701135)
- [18] E. Stringhini Junior, M.G.C. Dos Santos, L.B. Oliveira, M. Mercadé, MTA and biodentine for primary teeth pulpotomy: a systematic review and meta-analysis of clinical trials, *Clin Oral Investig.* (2018) 1-10. (DOI: 10.1007/s00784-018-2616-6)
- [19] M. Lipski, A. Nowicka, K. Kot, L. Postek-Stefańska, I. Wysoczańska-Jankowicz, L. Borkowski, P. Andersz, A. Jarzabek, K. Grocholewicz, E. Sobolewska, K. Woźniak, A. Drożdżik, Factors affecting the outcomes of direct pulp capping using Biodentine, *Clin. Oral Investig.* 22 (5) (2017) 2021-2029. (DOI: <https://doi.org/10.1007/s00784-017-2296-7>)

- [20] S.-K. Jun, J.-H. Lee, H.-H. Lee, The Biomineralization of a bioactive glass-incorporated light-curable pulp capping material using human dental pulp stem cells, *Biomed. Res. Int.* (2017) (DOI: <https://doi.org/10.1155/2017/2495282>)
- [21] Y. Yoshimine, K. Maeda, Histologic evaluation of tetracalcium phosphate-based cement as a direct pulp-capping agent, *Oral Surg. Oral Med. Oral Pathol. Oral Radiol.* 79 (30) (1995) 351-358. (DOI: [https://doi.org/10.1016/S1079-2104\(05\)80229-X](https://doi.org/10.1016/S1079-2104(05)80229-X)).
- [22] S. Kawashima, K. Shinkai, M. Suzuki, Effect of an experimental adhesive resin containing multi-ion releasing fillers on direct pulp-capping, *Dent Mater J.* 35 (3) (2016) 479–489. (DOI: [10.4012/dmj.2015-381](https://doi.org/10.4012/dmj.2015-381) JOI JST.JSTAGE/dmj/2015-381)
- [23] K. Ikemura, F.R. Tay, T. Endo, D.H. Pashley, A review of chemical-approach and ultramorphological studies on the development of fluoride-releasing dental adhesives comprising new pre-reacted glass ionomer (PRG) fillers, *Dent Mater J.* 27 (3) (2008) 315-339. (DOI: <https://doi.org/10.4012/dmj.27.315>)
- [24] N.S.W. Najma Hajira, N. Meena, GIOMER- The Intelligent Particle (New generation glass ionomer cement), *Int J Dent Oral Health*, 2 (4) (2015) (DOI: [10.16966/2378-7090.166](https://doi.org/10.16966/2378-7090.166))
- [25] Y. Fujimoto, M. Iwasa, R. Murayama, M. Miyazaki, A. Nagafuji, T. Nakatsuka, Detection of ions released from S-PRG fillers and their modulation effect, *Dent Mater J.* 29 (4) (2010) 392–397. (DOI: [:10.4012/dmj.2010-015](https://doi.org/10.4012/dmj.2010-015))

- [26] M. Yoneda, N. Suzuki, T. Hirofuji, Antibacterial effect of surface pre-reacted glass ionomer filler and eluate–mini review, *Pharm Anal Acta.* 6 (3) (2015) (DOI: 10.4172/2153-2435.1000349)
- [27] S. Saku, H. Kotake, R.J. Scougall-Vilchis, S. Ohashi, M. Hotta, S. Horiuchi, K. Hamada, K. Asaoka, E. Tanaka, K. Yamamoto, Antibacterial activity of composite resin with glass-ionomer filler particles, *Dent Mater J.* 29 (2) (2010) 193-198. (DOI: <https://doi.org/10.4012/dmj.2009-050>)
- [28] S. Imazato, Bio-active restorative materials with antibacterial effects: new dimension of innovation in restorative dentistry, *Dent Mater J.* 28 (1) (2009) 11-19. (DOI: <https://doi.org/10.4012/dmj.28.11>)
- [29] T. Miyauchi, Remineralization of the dentine decay by bioactive restoration material; *The Japanese Society of Conservative Dentistry* 52 (6) (2009) 469-482.
- [30] K. Asano, R. Kawamoto, M. Iino, T. Fruichi, K. Nojiri, T. Takamizawa, M. Miyazaki, Effect of pre-reacted glass-ionomer filler extraction solution on demineralization of bovine enamel, *Oper Dent.* 39 (2) (2014) 159-165. (DOI: 10.2341/13-034-L)
- [31] M. Ijima, K. Kawaguchi, N. Kawamura, S. Ito, T. Saito, I. Mizoguchi, The effects of single application of pastes containing ion-releasing particles on enamel demineralization, *Dent Mater J.* 36 (4) (2017) 461-468. (DOI:10.4012/dmj.2016-307)

- [32] A. A. Ratna, S. Triaminingsih, Y. K. Eriwat. The effect of prolonged immersion of giomer bulk-fill composite resin on the pH value of artificial saliva and resin surface roughness, *J. Phys.* 884 (2017) (DOI: 10.1088/1742-6596/884/1/012011)
- [33] M. Tamura, M. E. Cueno, K. Abe, N. Kamio, K. Ochiai, K. Imai. Ions released from a S-PRG filler induces oxidative stress in *Candida albicans* inhibiting its growth and pathogenicity, *Cell Stress Chaperones.* 23 (6) (2018) 1337-1343.
(<https://doi.org/10.1007/s12192-018-0922-1>).
- [34] G. Boivin, P. Deloffre, B. Perrat, G. Panczer, M. Boudeulle, Y. Mauras, P. Allain, Y. Tsouderos, P.J. Meunier, Strontium distribution and interactions with bone mineral in monkey iliac bone after strontium salt (S 12911) administration, *J. Bone Miner. Res.* 11 (9) (1996) 1302-1311. (DOI: 10.1002/jbmr.5650110915).
- [35] L. Mao, L. Xia, J. Chang, J. Liu, L. Jiang, C. Wu, B. Fang. The synergistic effects of Sr and Si bioactive ions on osteogenesis, osteoclastogenesis and angiogenesis for osteoporotic bone regeneration. *Acta. Biomater.* 61 (2017) 217-232. (DOI: 10.1016/j.actbio.2017.08.015).
- [36] L. Han, T. Okiji, Evaluation of the ions release / incorporation of the prototype S-PRG filler containing endodontic sealer, *Dent Mater J.* 30 (6) (2011) 898-903. (DOI: 10.4012/dmj.2011-101).

- [37] Y. Takahashi, M. Okamoto, S. Komichi, S. Imazato, T. Nakatsuka, S. Sakamoto, K. Kimoto, M. Hayashi, Application of a direct pulp capping cement containing S-PRG filler, *Clin Oral Investig.* (2018) 1-9. (DOI:10.1007/s00784-018-2596-6).
- [38] E. Shorter, The history of lithium therapy, *Bipolar Disord.* 11 (Suppl 2) (2009) 4–9. (DOI: 10.1111/j.1399-5618.2009.00706.x)
- [39] R. M. Vieiraa, H. K. Manjib, C. A. Zarate. The role of lithium in the treatment of bipolar disorder: convergent evidence for neurotrophic effects as a unifying hypothesis. *Bipolar Disord.* 11 (2) (2009) 92 – 109. (DOI: 10.1111/j.1399-5618.2009.00714.x).
- [40] F. Marmol. Lithium: Bipolar disorder and neurodegenerative diseases Possible cellular mechanisms of the therapeutic effects of lithium. *Prog. Neuropsychopharmacol. Biol. Psychiatry.* 32 (8) (2008) 1761-1771. (DOI: 10.1016/j.pnpbp.2008.08.012).
- [41] Li Li, X. Peng, Y. Qin, R. Wang, J. Tang, X. Cui, T. Wang, W. Liu, H. Pan, B. Li, Acceleration of bone regeneration by activating Wnt/ β -catenin signaling pathway via lithium released from lithium chloride/calcium phosphate cement in osteoporosis, *Sci. Rep.* 7:45204 (2017) (DOI: 10.1038/srep45204)
- [42] P.C. -Lacroix, M. Ai, F. Morvan, S.R. -Roman, B. Vayssiè`re, C. Belleville, K. Estrera, M.L. Warman, R. Baron, G. Rawadi, Lrp5-independent activation of Wnt signaling by lithium chloride increases bone formation and bone mass in mice, *Proc. Natl. Acad. Sci. U.S.A.* 102 (48) (2005) 17406–17411. (DOI: 10.1073/pnas.0505259102).

- [43] Y. Jin, L. Xu, X. Hu, S. Liao, J. L. Pathak, J. Liu. Lithium chloride enhances bone regeneration and implant osseointegration in osteoporotic conditions. *J Bone Miner. Metab.* 35 (5) (2017) 497 – 503. (DOI: 10.1007/s00774-016-0783-6).
- [44] K. Ishimoto, S. Hayano, T. Yanagita, H. Kurosaka, N. Kawanabe, S. Itoh, M. Ono, T. Kuboki, H. Kamioka, T. Yamashiro, Topical application of lithium chloride on the pulp induces dentin regeneration, *PLoS ONE*, 10 (3) (2015) e0121938. (DOI: 10.1371/journal.pone.0121938).
- [45] P. Han, S. Ivanovski, R. Crawford, Y. Xiao, Activation of the canonical wnt signaling pathway induces cementum regeneration, *J Bone Miner. Res.* 30 (7) (2015) 1160-1174. (DOI: 10.1002/jbmr.2445)
- [46] P. Han, C. Wu, J. Changb, Y. Xiao. The cementogenic differentiation of periodontal ligament cells via the activation of Wnt/ β -catenin signalling pathway by Li⁺ ions released from bioactive scaffolds, *Biomaterials* 33 (27) (2012) 6370-6379. (DOI: <https://doi.org/10.1016/j.biomaterials.2012.05.061>).
- [47] J. Pan, S. He, X. Yin, Y. Li, C. Zhou, S. Zou, Lithium enhances alveolar bone formation during orthodontic retention in rats, *Orthod. Craniofac. Res.* 20 (3) (2017) 146-151. (DOI: 10.1111/ocr.12190).
- [48] F. Liu, S.E. Millar, Wnt/B-catenin signaling in oral tissue development and disease, *J. Dent. Res.* 89 (4) (2010) 318-330. (DOI: 10.1177/0022034510363373).
- [49] L. Freland, J. M. Beaulieu. Inhibition of GSK3 by lithium, from single molecules to

- signaling networks. *Front. Mol. Neurosci.* 5 (14) (2012) (DOI: 10.3389/fnmol.2012.00014).
- [50] J. Wang, B. Liu, S. Gu, J. Liang. Effects of Wnt/ β -catenin signalling on proliferation and differentiation of apical papilla stem cells. *Cell Prolif.* 45 (2) (2012) 121-131. (DOI: 10.1111/j.1365-2184.2012.00806.x).
- [51] N. Han, Y. Zheng, R. Li, X. Li, M. Zhou, Y. Niu, Q. Zhang, β -catenin enhances odontoblastic differentiation of dental pulp cells through activation of Runx2, *Plos ONE* 9 (2) (2014) e88890. (DOI: 10.1371/journal.pone.0088890).
- [52] D.B. Bernkopf, M.V. Hadjihannas, J. Behrens, Negative-feedback regulation of the Wnt pathway by conductin /axin2 involves insensitivity to upstream signaling, *J. Cell Sci.* 128 (1) (2015) 33-39. (DOI:10.1242/jcs.159145).
- [53] L. Qian, J. P. Mahaffey, H. L. Alcorna, K. V. Anderson. Tissue-specific roles of Axin2 in the inhibition and activation of Wnt signaling in the mouse embryo. *Proc. Natl. Acad. Sci.* 108 (21) (2011) 8692–8697. (DOI: 10.1073/pnas.1100328108).
- [54] R. Babb, D. Chandrasekaran, V. Carvalho, M. Neves, P.T. Sharpe, Axin2-expressing cells differentiate into reparative odontoblasts via autocrine Wnt/ β -catenin signaling in response to tooth damage, *Sci. Rep.* 7 (3102) (2017) (DOI: 10.1038/s41598-017-031456).

- [55] M. G. Gandolfi, P. Taddei, A. Tinti and C. Prati. Apatite-forming ability (bioactivity) of ProRoot MTA. *Int. Endod. J.* 43 (2010) 917–929. (DOI: 10.1111/j.1365-2591.2010.01768.x).
- [56] M. Okamoto, Y. Takahashi, S. Komichi, M. Ali, N. Yoneda, T. Ishimoto, T. Nakano, M. Hayashi, Novel evaluation method of dentin repair by direct pulp capping using high-resolution micro-computed tomography, *Clin Oral Invest.* 22(8)(2018) 2879-2887. (DOI:10.1007/s00784-018-2374-5).
- [57] Y. Okamoto, Determination of fluorine in aqueous samples by electrothermal vaporisation inductively coupled plasma mass spectrometry (ETVICP-MS), *J. Anal. At. Spectrom.* 16 (2001) 539–5415. (DOI: 10.1039/b101969o).
- [58] W. Lin, L. Gao, W. Jiang, C. Niu, K. Yuan, X. Hu, R. Ma, Z. Huang, The role of osteomodulin on osteo/odontogenic differentiation in human dental pulp stem cells, *BMC Oral Health*, 19 (1) (22) (2019) (DOI: 10.1186/s12903-018-0680-6).
- [59] A.S. Hanak, L. Chevillard, S. El Balkhi, P. Risede, K. Peoch, B. Megarbane, Study of blood and brain lithium pharmacokinetics in the rat according to three different modalities of poisoning, *Toxicol. Sci.* 143 (1) (2014) 185–195. (DOI: 10.1093/toxsci/kfu224).
- [60] M. -J. Lee, J. -S. Kwona, J. -Y. Kimb, J. -H. Ryua, J. -Y. Seo, S. Jang, K. -M. Kima, C. -J. Hwangb, S. -H. Choi. Bioactive resin-based composite with surface pre-reacted glass-ionomer filler and zwitterionic material to prevent the formation of multi-

species biofilm. *Dent. Mater.* 35 (9) (2019) 1331-1341. (DOI:

<https://doi.org/10.1016/j.dental.2019.06.004>).

[61] S. Miki, H. Kitagawa, R. Kitagawa, W. Kiba, M. Hayashi, S. Imazato. Antibacterial activity of resin composites containing surface pre-reacted glass-ionomer (S-PRG)

filler. *Dent. Mater.* 32 (9) (2016) 1095-1102. (DOI:

<https://doi.org/10.1016/j.dental.2016.06.018>).

[62] M. Okamoto, M. Ali, S. Komichi, M. Watanabe, H. Huang, Y. Ito, J. Miura, Y. Hirose, M. Mizuhira, Y. Takahashi, D. Okuzaki, S. Kawabata, S. Imazato, M. Hayashi.

Surface pre-reacted glass filler contributes to tertiary dentin formation through a

mechanism different than that of hydraulic calcium-silicate cement. *J. Clin. Med.* 8

(1440) (2019) (DOI: 10.3390/jcm8091440).

[63] R. Machado-Vieira, H. K. Manjib, and C. A. Zarate Jr. The role of lithium in the treatment of bipolar disorder: convergent evidence for neurotrophic effects as a

unifying hypothesis. *Bipolar Disord.* 11 (2) (2009) 92-109. (DOI: :10.1111/j.1399

5618.2009.00714.x).

[64] S. Zung, F.L. Souza-Duran, M.G. Soeiro-de-Souza, R. Uchida, C.M. Bottino, G.F.

Busatto and H. Vallada. The influence of lithium on hippocampal volume in elderly

bipolar patients: a study using voxel-based morphometry. *Transl. Psychiatry.* 6 (6)

(2016) e864. (DOI: 10.1038/tp.2016.97).

- [65] M. Bark, O. Dandash, R. Daglas, S.M. Cotton, K. Allott, A. Fornito, C. Suo, P. Klauser, B. Liberg, L. Henry, C. Macneil, M. Hasty, P. McGorry, C. Pantelis and M. Yücel. Neuroprotection after a first episode of mania: a randomized controlled maintenance trial comparing the effects of lithium and quetiapine on grey and white matter volume. *Transl. Psychiatry*. 7 (2017) e1011. (DOI: 10.1038/tp.2016.281).
- [66] H. Su, Q. Yuan, D. Qin, X. Yang, W.M. Wong, K. F. So and W. Wu. Lithium enhances axonal regeneration in peripheral nerve by inhibiting glycogen Synthase kinase-3 β activation. *BioMed Res. Int.* (2014) (DOI: <http://dx.doi.org/10.1155/2014/658753>).
- [67] S. Gao, Y. Wang, X. Wang, P. Lin and M. Hu. Effect of lithium ions on cementoblasts in the presence of lipopolysaccharide in vitro. *Exp. Ther. Med.* 9 (4) (2015) 1277-1282. (DOI: 10.3892/etm.2015.2276).
- [68] T. Todd, Z. Lu, J. Zhao, B. Cline, W. Zhang, H. Chen, A. Kumar, W. Jiang, F. West, S. Franklin, L. Zheng and J. Xie. LiF@SiO₂ nanocapsules for controlled lithium release and osteoarthritis treatment. *Nano Res.* 11 (10) (2018) 5751–5760. (DOI: <https://doi.org/10.1007/s12274-018-2061-5>).
- [69] V. S. Gallicchio. Lithium effects on stem cells - advances in stem cell application in clinical medicine. *Adv. Cell Sci. Tissue Cul.* 2 (1) (2018) 14-24. (DOI: 10.35841/cell-science.2.1.1-11).

- [70] R. Fu, Y. Tang, Z. M. Ling, Y. Q. Li, X. Cheng, F. H. Song, L.H. Zhou and W. Wu. Lithium enhances survival and regrowth of spinal motoneurons after ventral root avulsion. *BMC Neuroscience*. 15 (84) (2014) (DOI: <http://www.biomedcentral.com/1471-2202/15/84>).
- [71] X. Huang, D.Y. Wu, G. Chen, H. Manji and D. F. Chen. Support of retinal ganglion cell survival and axon regeneration by lithium through a Bcl-2–dependent mechanism. *Investig. Ophthalmol. Vis. Sci.* 44 (1) (2003) 347-354. (DOI: <https://doi.org/10.1167/iovs.02-0198>).
- [72] C. Yu, P. V. Abbott, An overview of the dental pulp: its functions and responses to injury, *Aust. Dent. J.*, 27 (1) (2007) 4-16. (DOI: 10.1111/j.1834-7819.2007.tb00525.x).
- [73] N. Six, J. J. Lasfargues and M. Goldberg. In vivo study of the pulp reaction to Fuji IX, a glass ionomer cement. *J Dent.* 28 (6) (2000) 413-22. (DOI:10.1016/s0300-5712(00)00015-4).
- [74] E. M. Knijff, M.N. Breunis, R. W. Kupka, H. J. Wit, C. Ruwhof, G. W. Akkerhuis, W. A. Nolen, H. A. Drexhage. An imbalance in the production of IL-1b and IL-6 by monocytes of bipolar patients: restoration by lithium treatment. *Bipolar Disord.* 9 (7) (2007) 743–753. (DOI: 10.1111/j.1399-5618.2007.00444.x).
- [75] A. Nassar and A. N. Azab. Effects of lithium on inflammation. *ACS Chem Neurosci.* 5 (6) (2014) 451–458. (DOI: 10.1021/cn500038f).

- [76] S. Nahman, R. H. Belmaker and A. N. Azab. Effects of lithium on lipopolysaccharide-induced inflammation in rat primary glia cells. *Innate Immun.* 18 (3) (2012) 447–458. (DOI: 10.1177/1753425911421512).
- [77] H. M. Wang, T. Zhang, Q. Li, J. K. Huang, R. F. Chen and X.J. Sun. Inhibition of glycogen synthase kinase-3 β by lithium chloride suppresses 6-hydroxydopamine-induced inflammatory response in primary cultured astrocytes. *Neurochem. Int.* 63 (5) (2013) 345–353. (DOI: 10.1016/j.neuint.2013.07.003).
- [78] S. Vahabzadeh, V.K. Hack, S. Bose, Lithium-doped β -tri-calcium phosphate: Effects on physical, mechanical and in vitro osteoblast cell–material interactions, *J. Biomed. Mater. Res. Part B* 105 (2) (2015)391-399. (DOI: 10.1002/jbm.b.33485).
- [79] F. Liu, E. Y. Chu, B. Watt, Y. Zhang, N. M. Gallant, T. Andl, S. H. Yang, M. M. Lu, S. Piccolo, R. S. Ullrich, M. M. Taketo, E. E. Morrisey, R. Atit, A. A. Dlugosz, S. E. Millar. Wnt/ β -catenin signaling directs multiple stages of tooth morphogenesis. *Dev. Biol.* 313 (1) (2008) 210-224. (DOI: 10.1016/j.ydbio.2007.10.016).
- [80] R.S. Jope, Lithium and GSK-3: one inhibitor, two inhibitory actions, multiple outcomes, *Trends Pharmacol. Sci.* 24 (9) (2003) 441-443. (DOI: [https://doi.org/10.1016/S0165-6147\(03\)00206-2](https://doi.org/10.1016/S0165-6147(03)00206-2)).
- [81] E.-H. Jho, T. Zhang, C. Domon, C.-K. Joo, J.-N. Freund, F. Costantini, Wnt/ β -Catenin/Tcf signaling induces the transcription of Axin2, a negative regulator of the

- signaling pathway, *Mol. Cell. Biol.* 22 (4) (2002) 1172–1183. (DOI: 10.1128/MCB.22.4.1172–1183.2002).
- [82] M. Furuhashi, K. Yagi, H. Yamamoto, Y. Furukawa, S. Shimada, Y. Nakamura, A. Kikuchi, K. Miyazono and M. Kato. Axin facilitates Smad3 activation in the transforming growth factor β signaling pathway. *Mol. Cell. Biol.* 21 (2001) 5132–5141. (DOI: 10.1128/MCB.21.15.5132–5141.2001).
- [83] J. Y. Leung, F. T. Kolligs, R. Wu, Y. Zhai, R. Kuick, S. Hanash, K. R. Cho and E. R. Fearon. Activation of AXIN2 Expression by β -Catenin-T Cell Factor. A feedback repressor pathway regulating Wnt signaling. *J. Biol. Chem.* 277 (24) (2002) 21657–21665. (DOI: 10.1074/jbc.M200139200).
- [84] L. Niu, K. Jiao, T. Wang, W. Zhang, J. Camilleri, B. E. Bergeron, H. Feng, J. Mao, J. Chen, D. H. Pashley and F. R. Tay, A review of the bioactivity of hydraulic calcium silicate cements, *J Dent.*, 42(5) (2014) 517–533. (Doi:10.1016/j.jdent.2013.12.015).
- [85] E. A. Bortoluzzi, N. J. Broon, C. M. Bramante, R. B. Garcia, I. G. Moraes and N. Bernardineli, Sealing ability of MTA and radiopaque portland cement with or without calcium chloride for root-end filling, *J Endod.*, 32 (9) (2006) 897-900. (DOI:10.1016/j.joen.2006.04.006).
- [86] R Abimanyu, R Meidyawati and Kamizar. Differences in microleakage between MTA and Biodentine™ as material for treatment of access perforation, *J. Phys. Conf. Ser.* 884 (2017) (DOI: 10.1088/1742-6596/884/1/012104).

- [87] S. Sadr, A. Golmoradzadeh, M. Raoof, M. J. Tabanfar. Microleakage of single-cone gutta-percha obturation technique in combination with different types of sealers, Iran Endod J., 10 (3) (2015) 199-203. (DOI: 10.7508/iej.2015.03.011).
- [88] D. F. Smith, K. Thomsen, Renal lithium clearance in adrenalectomized rats, Am. J. Physiol. 225 (1) (1973) 159-161.
- [89] W. Young. Review of Lithium Effects on Brain and Blood. Cell Transplantation. 8 (2009) 951-975. (DOI: 10.3727/096368909X471251).
- [90] M. Gitlin. Lithium side effects and toxicity: prevalence and management strategies. Int J Bipolar Disord. 4 (27) (2016) (DOI: 10.1186/s40345-016-0068-y).

4. Funds and grants

1. This study was partly supported by grants from JSPS KAKENHI (JP#16K20453, #17K11704, #17H06848, #19K18995).
2. Grant for research activities was obtained from the Department of Research and Development- SHOFU Inc. (J#170803029).

5. Published articles

As a first author:

Authors names: Manahil Ali, Motoki Okamoto, Shungo Komichi, Masakatsu Watanabe, Hailing Huang, Yusuke Takahashi, Mikako Hayashi.

Title: Lithium-containing surface pre-reacted glass fillers enhance Hdpsc functions and induce reparative dentin formation in a rat pulp capping model through the activation of Wnt/ β -catenin signaling.

Journal name: Acta Biomaterialia journal

Volume and pages: 96: 594–604 (2019)

Date: Received 8 February 2019, Revised 6 June 2019, Accepted 13 June 2019, Available online 15 June 2019.

DOI: <https://doi.org/10.1016/j.actbio.2019.06.016>

This illustration summarizes and explains the possible mechanism of action of S-PRG/Li-100 mM that can activate Wnt/ β -catenin signaling pathway in the odontoblastic cell layer adjacent to the exposure area. Lithium ions may act as a Wnt ligands and bind to LRP5/6 receptor to start signaling transductions where Dishivilled (Dsh) protein activated, and also inhibit the phosphorylation of GSK-3 β and hence prevent the phosphorylation and degradation of β -catenin through inhibiting the function of the β -catenin destruction complex that also include Axin2 and Adeno-polyposis coli (APC). Hypo-phosphorylated β -catenin can accumulate in the cytoplasm and translocate into the nuclei, then form a complex with T-cell Factor/Lymphoid enhancing factor (TCF/LEF) and transcribe the target genes and initiate different cell functions. Activated odontoblastic-like cells in early stages resulted in tertiary dentin formation 28-days post capping.

6. Academic presentations:

1. Manahil.S.Ali, Okamoto.M, Watanabe.M, Huang Hailing, Takahashi.Y, Hayashi.M. Antibacterial activity of lithium-containing S-PRG fillers against *Streptococcus mutans* biofilm. The UAE International Dental Conference & Arab Dental Exhibition (AEEDC-Dubai), UAE, February 2020 (Digital poster presentation).
2. Manahil.S.Ali, Okamoto.M, Komichi.S, Watanabe.M, Huang Hailing, Takahashi.Y, Hayashi.M. Bioactivity and biocompatibility of lithium-contained surface pre-reacted glass fillers. International Association for Dental Research/Pan European Regions (IADR/PER) General Session, Vancouver, Canada, July 2019 (Poster presentation).
3. Manahil.S.Ali, Okamoto.M, Komichi.S, Watanabe.M, Huang Hailing, Takahashi.Y, Hayashi.M. Lithium containing S-PRG fillers enhanced tertiary dentin formation via Wnt/ β -catenin pathway activation. International Federation of Endodontic Associations (IFEA), Seoul, Korea. October 2018 (Oral presentation).
4. Manahil.S.Ali, Okamoto.M, Komichi.S, Watanabe.M, Takahashi.Y, Hayashi.M. Lithium Ions Contained S-PRG fillers facilitated hDPSCs migration and functional vascularity. International Association for Dental Research/Pan European Regions (IADR/PER) General Session, London, UK. July 2018 (oral presentation).
5. Manahil.S.Ali, Okamoto.M, Komichi.S, Watanabe.M, Takahashi.Y, Hayashi.M. Effects of S-PRG fillers containing Li ions on the function of pulp cells. Japanese Society of Conservative Dentistry/Korean Academy of Conservative Dentistry (JSCD/KACD) Annual Meeting, Morioka, Japan, October 2017 (oral presentation).
6. Manahil.S.Ali, Okamoto.M, Komichi.S, Takahashi.Y, Ito.Y, Hayashi.M. Application of S-PRG cement containing Li-ions as a direct pulp capping material. Japanese Society of Conservative Dentistry (JSCD) Annual Meeting, Aomori, Japan, June 2017 (poster presentation).

Chapter V

Figures and tables

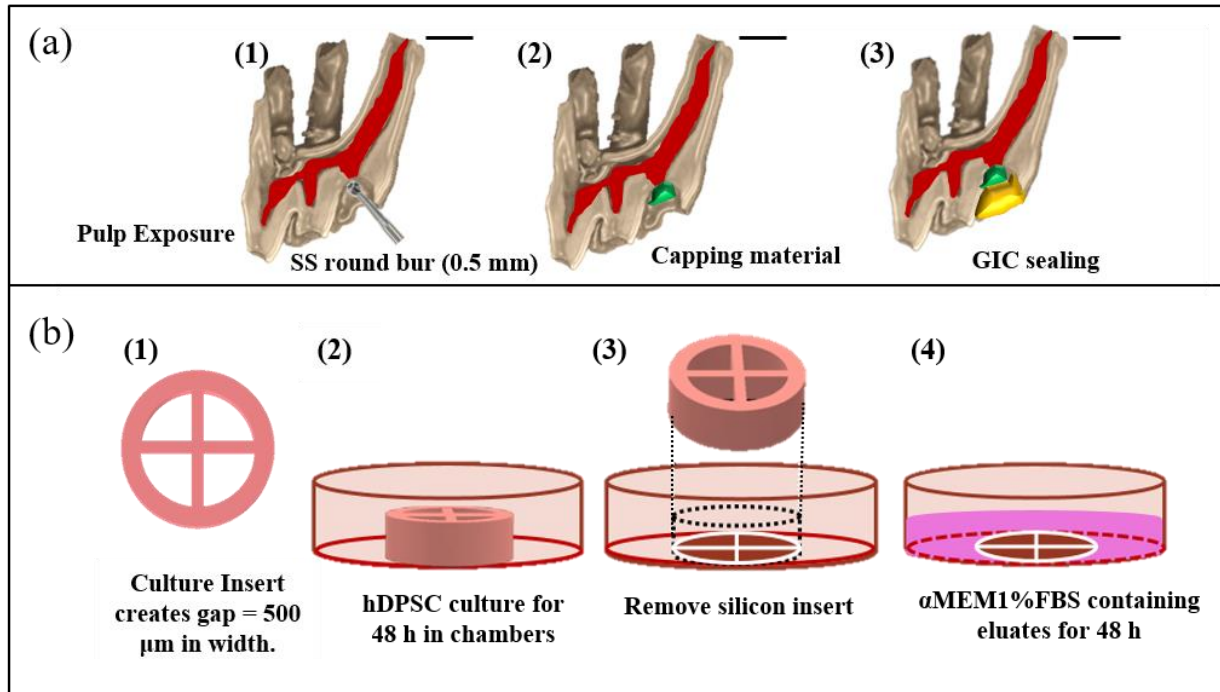


Figure 1(a) Schematic of pulp capping experiment. A bowl-shaped cavity was prepared in the mesial fossa of the maxillary first molar using a stainless steel (SS) round bur of 0.5 mm in diameter with a pulp exposure < 0.2 mm in diameter (1). The exposed pulp was capped with a pulp capping material (green) (2). The cavity was sealed using glass ionomer cement (GIC; yellow) (3). Scale bar = 1 mm. **Fig. 1(b) Cell migration assay protocol using an ibidi culture insert.** The inserts can create a gap of 500 μm (1). When placed into 60-mm dishes, human dental pulp stem cells (hDPSCs) were cultured in the four wells for 48 h (2). The culture insert was removed (3) and hDPSCs were additionally cultured in the media containing the experimental eluates for another 48 h (4). The eluates were prepared by immersing each cement in distilled water for 7 days.

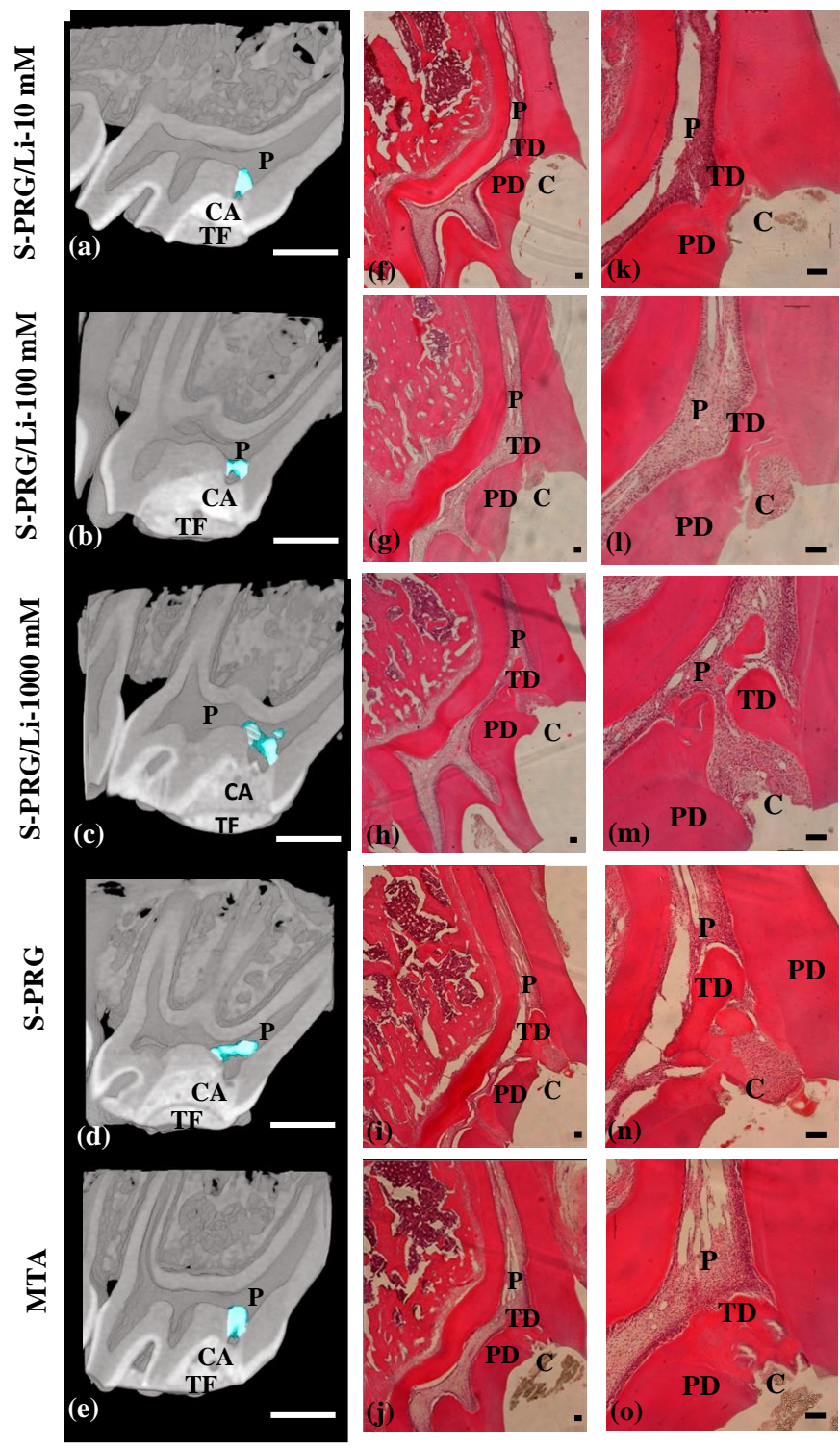


Figure. 2. Micro-CT and histopathological evaluation of different pulp capping

materials. Micro-CT images analyzed by TRI 3D BON software, displaying the area of tertiary dentin formed in response to different pulp-capping materials (TD in blue) 28-days post capping (2a-2e). H&E stained sections (5 μ m thick) (2f-2j). H&E staining at higher magnification (2k-2o) showed the new tertiary dentin (TD) that formed beneath the exposure site. S-PRG/Li-10 and S-PRG/Li-100 mM showed a complete dentin bridge similar to MTA (2k, 2l and 2o), while S-PRG/Li-1000 mM resulted in an incomplete bridge and S-PRG displayed a defected bridge (n). (P: pulp, CA: capping agent, TF: temporary filling, TD: tertiary dentin, PD: primary dentin, C: cavity, Scale bar of micro CT images= 1 mm, H and E stained section of higher magnification= 0.1 mm, higher magnification=100 μ m, n=5).

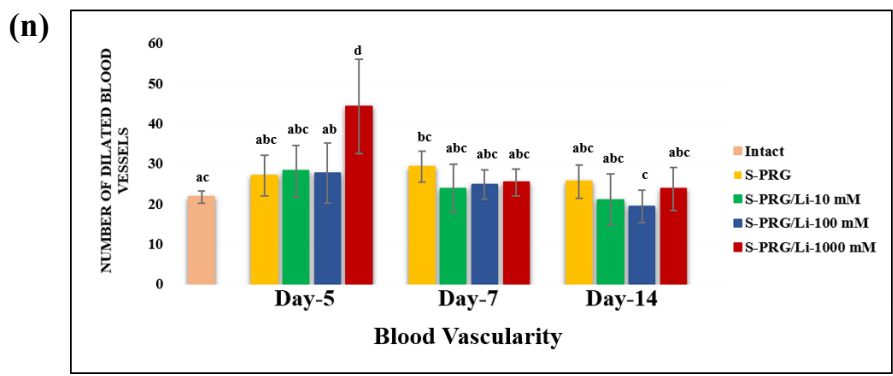
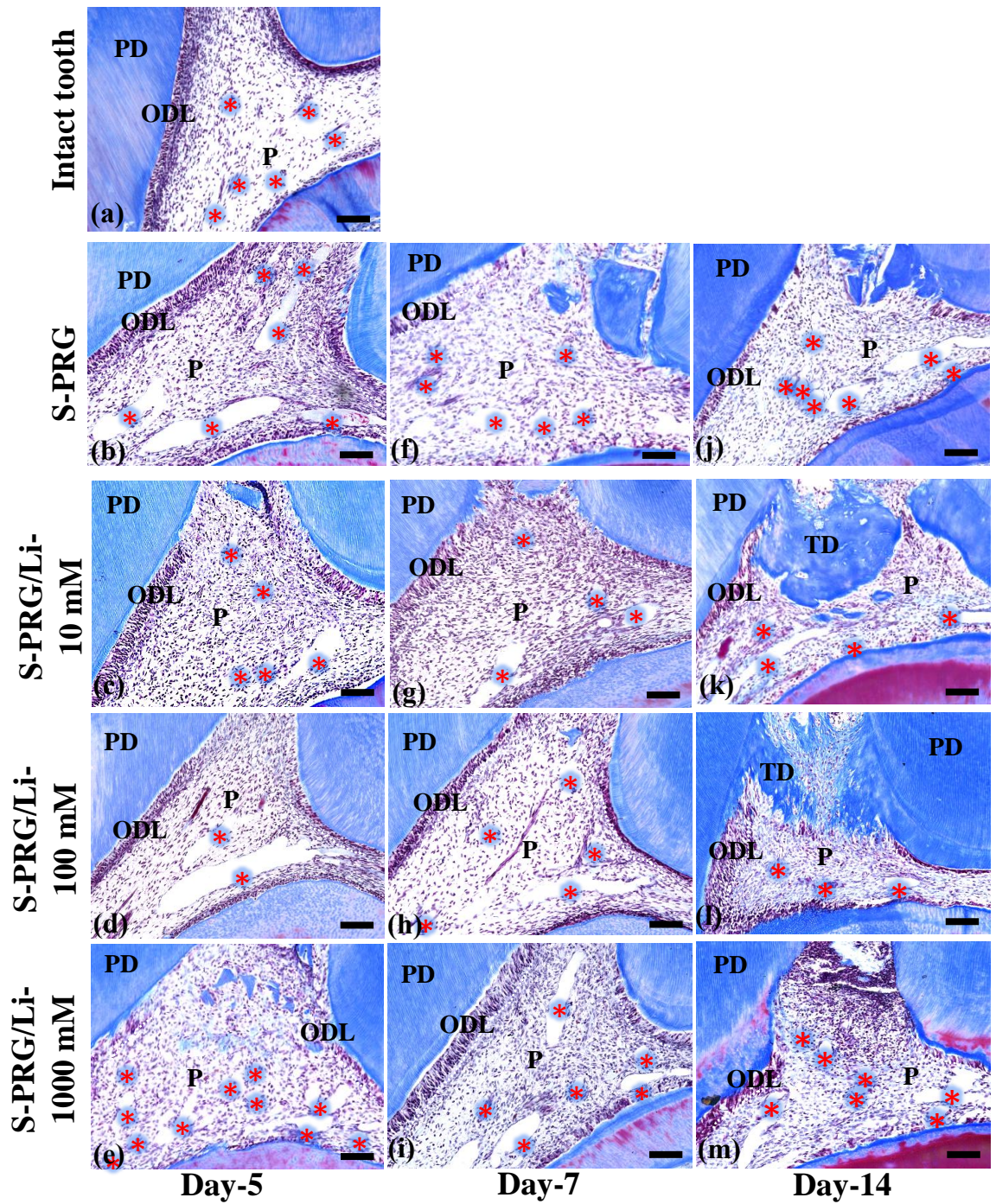


Figure 3. Masson trichrome staining micrographs. The control sample used in this study was the intact tooth sample below the mesial horn region (3a). Results of day-5 (3b-3e), day-7 (3f-3i) and day-14 (3j-3m) show the existence of dilated blood vessels (indicated with red asterisk) beneath the exposure site, suggesting active inflammation or the dentinogenesis process (Scale bar = 100 μ m). From the control intact specimens, similar distribution to S-PRG, S-PRG/Li-10 and S-PRG/Li-100 mM was observed. However, more vessels were demonstrated in the S-PRG/Li-1000 mM specimens. The quantitative data of the blood vessels number beneath the capping region, along with the mesial canal, have been shown in the bar graph (n) (n=3, $p < 0.05$. Same alphabets mean no statistical significant difference. P: Pulp, ODL: Odontoblastic layer, PD: Primary dentin, TD: Tertiary dentin).

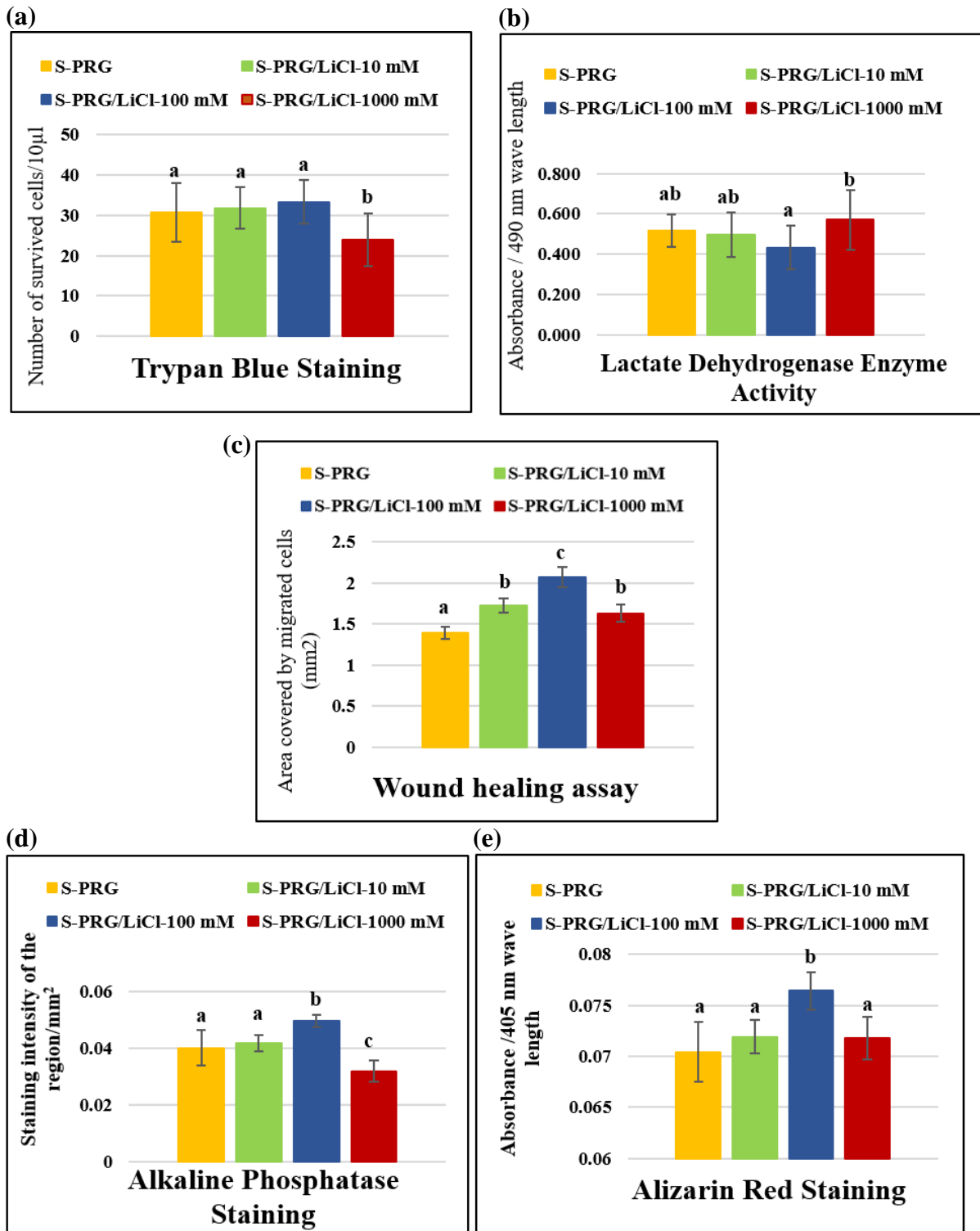


Figure 4. *In vitro* cell studies outcomes. The results show changes in cell phenotype after exposure to the eluates from S-PRG cements containing various concentrations of LiCl. Cell proliferation results after Trypan blue staining procedure indicated that S-PRG/Li-100 mM

maintained the growth of the cells compared to S-PRG/Li-1000 mM (4a). Lactate dehydrogenase (LDH) enzyme activity indicates cytotoxicity of the cement (4b). The results of LDH showed that S-PRG/Li-100 mM was not cytotoxic, when compared to the results of the control group. Cell migration (quantified by Image J) results indicate a higher number of migrated cells in cells that were cultured in S-PRG/Li-100 mM (4c). Alkaline phosphatase (ALP) staining (evaluated by Image J) (4d) and the absorbance of dissolved crystals after staining with Alizarin Red staining (4e) show that S-PRG/Li-100 mM could facilitate the HDPSCs differentiation and mineralization, respectively. (n=3, significance was indicated by different letters a, b, c and d, $p < 0.05$).

Figure 5

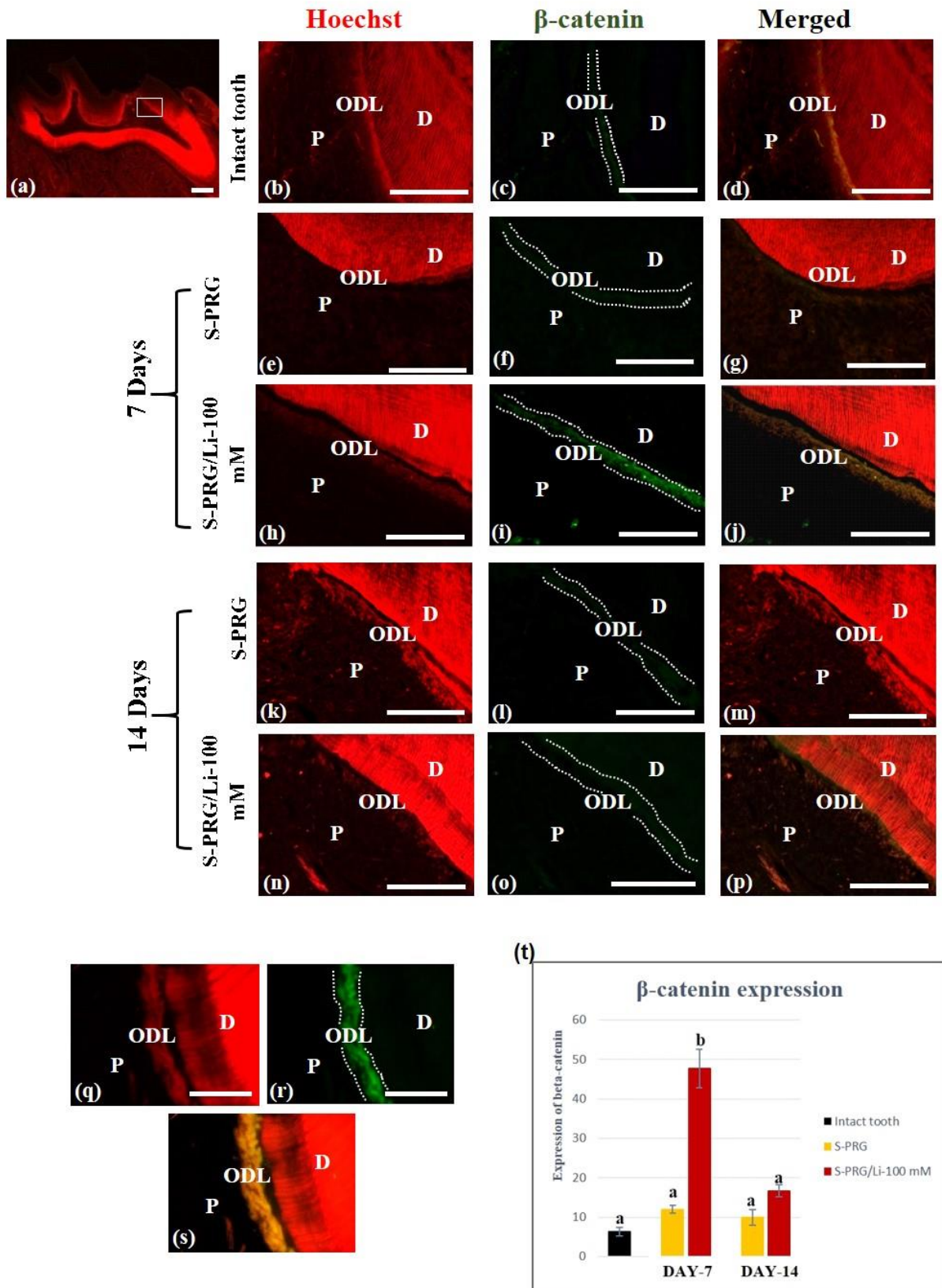


Figure 5. Immunofluorescent expression of β -catenin at the odontoblastic cell layer.

Low-power magnification shows the target areas of β -catenin expression beneath the cavity (5a). Micrographs show β -catenin expression in the odontoblastic cell layer in the intact tooth structure (5b-5d) and after pulp capping with S-PRG (5e-5g, 5k-5m) and S-PRG/Li-100 mM at 7- and 14-days (5h-5j, 5n-5p) post-operatively. Strong expression was observed in the S-PRG/Li-100 mM group 7-days post-operatively, that declined by day-14. The S-PRG group displayed similar expression as that displayed by the control group at both experimental time points. Higher magnification images show the translocation of β -catenin into the nuclei of odontoblastic cells in S-PRG/Li-100 mM samples at 7-days post-operatively (5q-5s). Quantitated values of β -catenin expression levels using three randomly selected samples from each group (n=3), significance indicated by different letters a and b, $p < 0.05$). (P: pulp, ODL: odontoblastic cell layer, D: dentin, Scale bar =100 μ m).

Figure 6

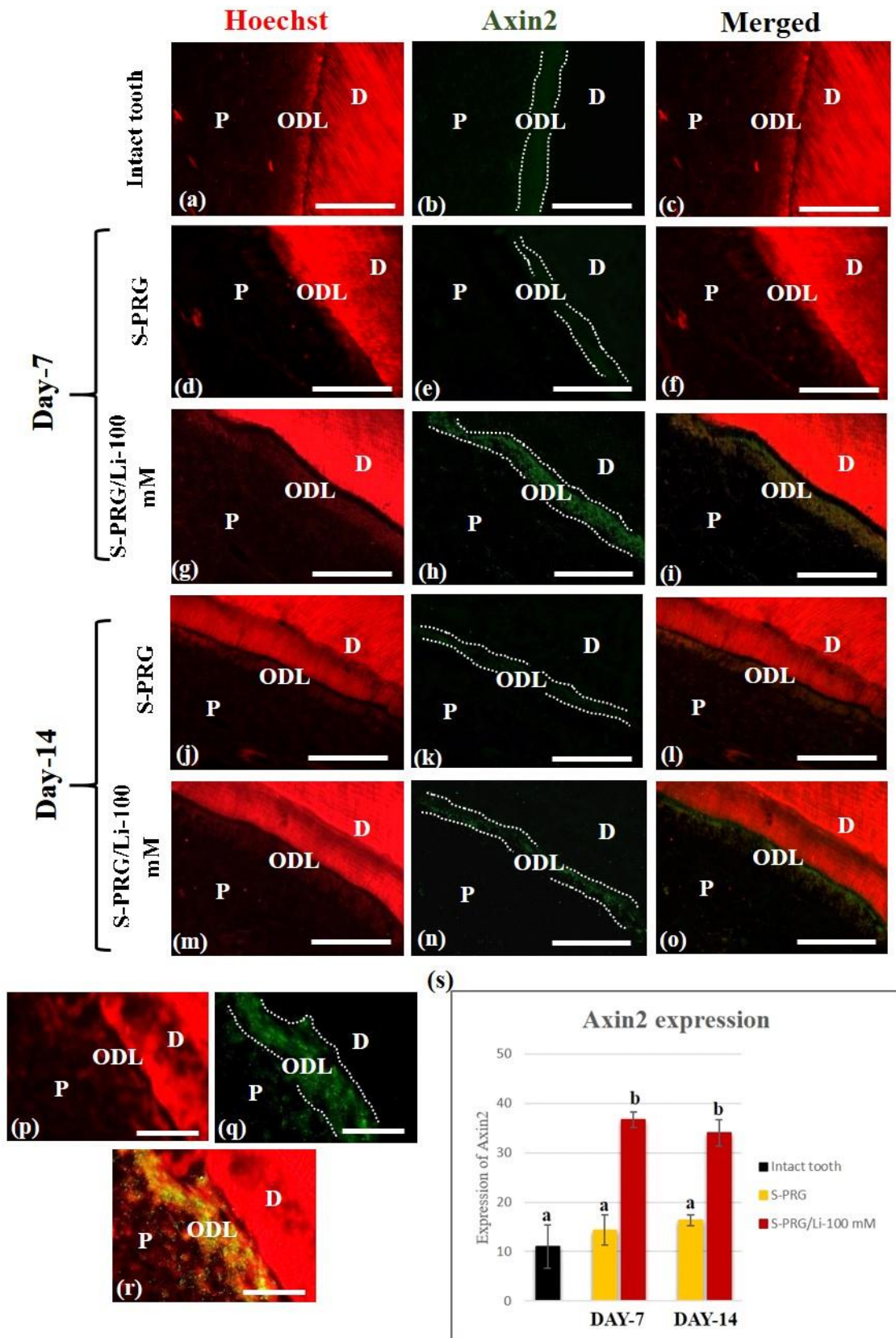


Figure 6. Immunofluorescent expression of Axin2 at the odontoblastic cell layer. S-PRG (6d-6f, 6j-6i) and S-PRG/Li-100 mM (6g-6i, 6m-6o) were compared to the specimens of the control group (6a-6c) 7- and 14- days post-operatively (6a-6o). S-PRG/Li-100 mM specimens expressed Axin2 continuously at both time points (6g-6i, 6m-6o), when the S-PRG group showed weak expression of Axin2, similar to that presented by the control group (6a-6f, 6j-6i). A diffuse pattern of Axin2 expression in higher magnification images following treatment with S-PRG/Li-100 mM for 7 days was observed (6p-6r). Quantitated values of Axin2 expression (6s). (n=3, significance indicated by different letters a and b, $p < 0.05$. P: pulp, ODL: odontoblastic cell layer, D: dentin. Scale bar =100 μ m).

Figure 7

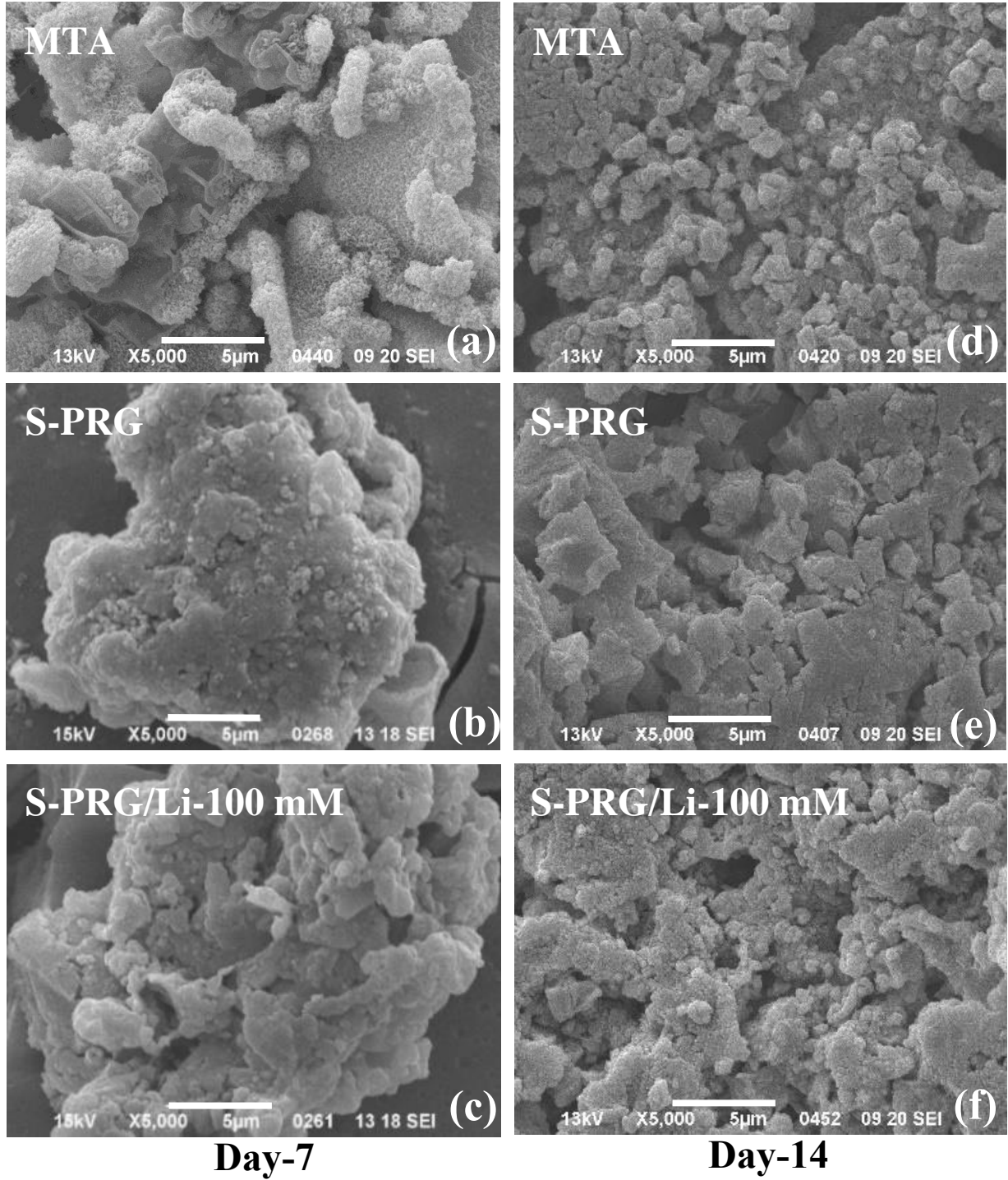


Figure 7. Hydroxy-apatite formation on the surface of different cement disks incubated in simulated body fluid (SBF). Micrographs show the apatite-like structures formed on the surfaces of MTA, S-PRG, and S-PRG/Li-100 mM, following 7 days, immersed in SBF (7a, 7b and 7c). MTA groups presented rod-like structures as compared to micrographs presented by other groups, that displayed irregular structures that were formed by aggregation of other apatite. 14 days (7d, 7e and 7f) after immersion into the SBF, they coalesced to form a layer of apatite on the surface of the disks (n= 3, Scale bar = 5 μ m).

Figure 8

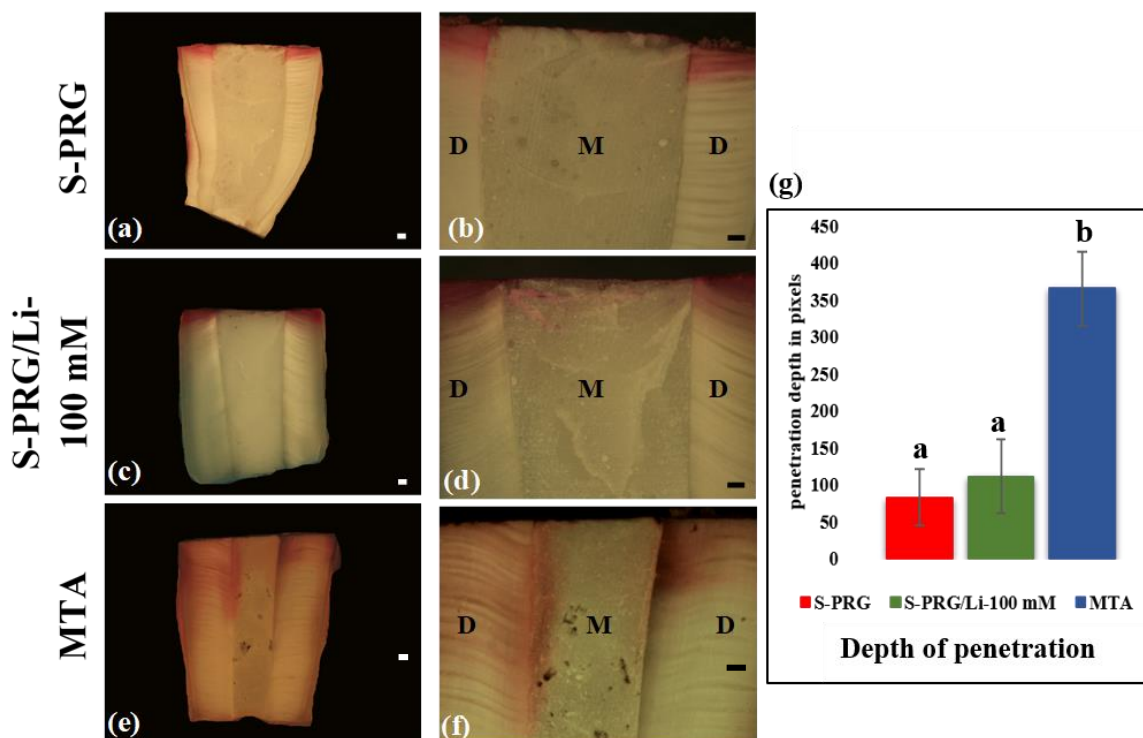


Figure 8. Dye penetration test results. Bovine teeth filled with different cements were soaked in 0.1% rhodamine-B solution for 24 hours. The results of S-PRG (8a and 8b) and S-PRG/Li-100 mM (8c and 8d) showed less depth of dye penetration compared to MTA (8e and 8f), that demonstrated higher depths of penetration in many specimens, showing superiority of the S-PRG groups to MTA in terms of micro-leakage prevention. Quantitative data shows the depths of penetration in different groups in pixels (8g). (n=8, $p < 0.05$, scale bar = 100 pixels. D: Dentin, M: Material).

Figure 9

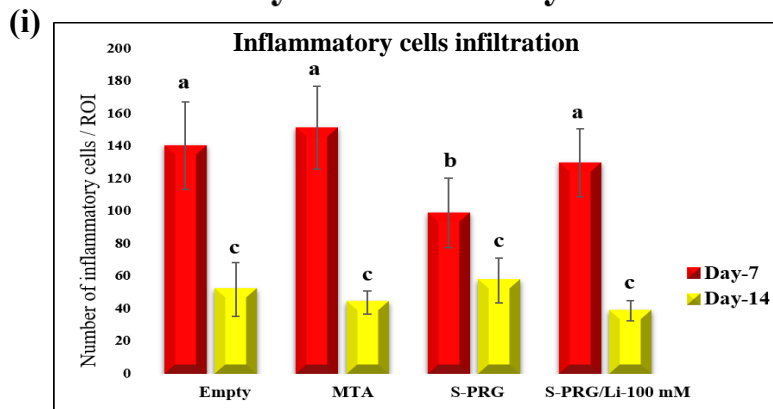
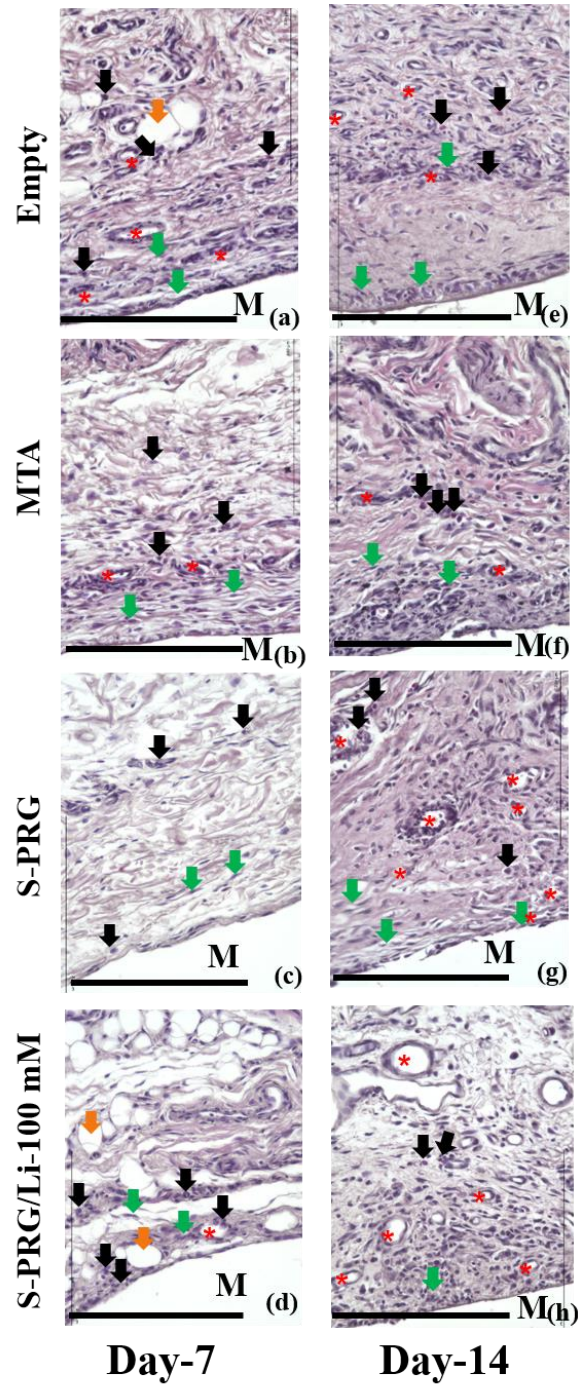


Figure 9. Inflammatory response to subcutaneous tissue implantation test. H and E stained micrographs were taken from the edges that faced the material from the tube. Empty samples represented the control group (9a and 9e), MTA (9b and 9f), S-PRG (9c and 9g), and S-PRG/Li-100 mM (9d and 9h). Tissues show some inflammatory cells (black arrow), blood vessels (red asterisk), fibroblasts (green arrow), and adipocytes (orange arrow). M: Material face. Quantitative data of inflammatory cells (i). Day-7 samples showed significantly lower inflammation in the S-PRG group that did not contain LiCl compared to the other groups. At day-14, all the experimental groups showed significant decrease from the day-7 samples and no significance was observed among any groups at day-14 (scale bar = 200 μm . n=4, $p < 0.05$).

Table 1 Compositions of surface pre-reacted glass (S-PRG) fillers and liquids. Mixing

ratio is 1.5/1.0 wt (P/L) for 40 seconds. Setting time is 90 seconds.

Powder	Components of the liquid part
S-PRG filler (Multifunctional glass fillers)	Copolymer of Acrylic acid and Tricarboxylic acid, Water, Others, <u>No LiCl</u> (PH < 1)
	Copolymer of Acrylic acid and Tricarboxylic acid, Water, <u>LiCl (10 mM)</u> , Others (pH < 1)
	Copolymer of Acrylic acid and Tricarboxylic acid, Water, <u>LiCl (100 mM)</u> , Others (pH < 1)
	Copolymer of Acrylic acid and Tricarboxylic acid, Water, <u>LiCl (1000 mM)</u> , Others (pH < 1)
MTA (Tri-calcium silicate, di-calcium silicate, tri-calcium aluminate, bismuth oxide, and calcium sulfate)	DW

Table 2 Mechanical properties of the cements used in this study. (Means \pm

SD) in MPa, n=5, * $p < 0.05$.

Cement	S-PRG	S-PRG/Li- 10 mM	S-PRG/Li- 100 mM	S-PRG/Li- 1000 mM
Compressive strength (MPa) n=5	70 \pm 7	65 \pm 7	52 \pm 7*	46 \pm 4*
Shear bond strength to dentin (MPa) n=5	1.7 \pm 0.3	1.9 \pm 0.8	1.9 \pm 0.4	1.3 \pm 0.2

Table 3 Ions leached from different cements used in this study.
(Means \pm SD), n=3, (DW: distilled water).

Cement	S-PRG	S-PRG/Li- 10 mM	S-PRG/Li- 100 mM	S-PRG/Li- 1000 mM
Released ions (mmol) {*DW, 37°C}	Li	0.0 \pm 0.0	0.1 \pm 0.0	1.9 \pm 0.3
	Si	1.7 \pm 0.1	1.7 \pm 0.1	1.8 \pm 0.1
	Al	0.8 \pm 0.1	0.7 \pm 0.1	0.9 \pm 0.1
	Sr	0.1 \pm 0.0	0.1 \pm 0.0	0.2 \pm 0.0
	B	58.6 \pm 4.7	58.4 \pm 5.4	59 \pm 5.6
	Na	7.5 \pm 2.2	7.5 \pm 2.1	8.1 \pm 2.3
	F	5.7 \pm 0.4	5.7 \pm 0.2	5.8 \pm 0.0
				2.4 \pm 0.1
				1.7 \pm 0.1
				1.4 \pm 0.1
				60 \pm 6.0
				9.9 \pm 3.2
				6.5 \pm 0.3

Table 4 The components of Simulated Body Fluid (SBF) to prepare 1 L of solution.

Component	Amount
NaCl	8.035 g
NaHCO₃	0.355 g
KCl	0.225 g
K₂HPO₄·3H₂O	0.231 g
MgCl₂·6H₂O	0.311 g
1M-HCl	39 ml
CaCl₂	0.292 g
Na₂SO₄	0.072 g
(CH₂OH)₃CNH₂	6.118 g